

Effects of vutrisiran on cardiac structure and function in patients with transthyretin amyloidosis with cardiomyopathy: secondary outcomes of the HELIOS-B trial

Received: 3 February 2025

Accepted: 10 June 2025

Published online: 06 August 2025

 Check for updates

Karola S. Jering¹, Marianna Fontana², Olivier Lairez³, Simone Longhi⁴, Olga Azevedo⁵, Caroline Morbach^{6,7}, Shaun Bender⁸, Patrick Y. Jay⁸, John Vest⁸, Bernard E. Bulwer¹, Narayana Prasad¹, Scott D. Solomon¹✉ & Hicham Skali¹

In the HELIOS-B randomized clinical trial, the RNA interference therapeutic agent vutrisiran reduced the risk of all-cause mortality and recurrent cardiovascular events among patients with transthyretin amyloidosis with cardiomyopathy (ATTR-CM). In this secondary analysis of HELIOS-B, we evaluated vutrisiran's effects on echocardiographic measures of cardiac structure and function in patients with ATTR-CM receiving vutrisiran or placebo ($n = 654$, 93% men). At 30 months after treatment, as compared to the placebo group, vutrisiran treatment attenuated increases in mean left ventricular (LV) wall thickness (least squares mean difference: -0.4 mm; 95% confidence interval (CI): -0.8 , 0.0 ; $P = 0.03$) and LV mass index (-10.6 g m⁻²; 95% CI: -18.0 , -3.3 ; $P < 0.01$). Vutrisiran treatment also attenuated declines in LV ejection fraction (2.0%; 95% CI: 0.3 , 3.7 ; $P = 0.02$), absolute global longitudinal strain (1.2%; 95% CI: 0.7 , 1.7 ; $P < 0.01$) and LV stroke volume (4.1 ml; 95% CI: 1.7 , 6.4 ; $P < 0.01$), and decreased both the average ratio of early diastolic transmitral flow velocity to early diastolic mitral annular tissue velocity (-2.0 ; 95% CI: -2.9 , -1.2 ; $P < 0.01$) and the early to late diastolic transmitral flow velocities ratio (-0.3 ; 95% CI: -0.6 , -0.0 ; $P = 0.04$), as compared to placebo. Consistent with its clinical benefits, these echocardiographic findings indicate favorable effects of vutrisiran on cardiac structure and function in patients with ATTR-CM. ClinicalTrials.gov registration: [NCT04153149](https://clinicaltrials.gov/ct2/show/study/NCT04153149).

Transthyretin amyloidosis with cardiomyopathy (ATTR-CM) is an increasingly recognized cause of heart failure (HF) associated with high morbidity and mortality. ATTR-CM is caused by extracellular accumulation of misfolded transthyretin (TTR) in the form of amyloid fibrils in the heart, leading to restrictive physiology, conduction disease and arrhythmias. Infiltration of the myocardium with amyloid fibrils also underlies the characteristic findings of increased ventricular wall thickness, diastolic dysfunction with elevated filling pressures, biatrial

enlargement, decreased global longitudinal strain (GLS) with relative apical sparing and, at advanced stages, impairment of left ventricular ejection fraction (LVEF)^{1,2}. Echocardiography is used for diagnostic purposes and in conjunction with clinical status and cardiac biomarkers as a tool to monitor disease progression^{3–5}.

Vutrisiran, a subcutaneously administered RNA interference therapeutic agent, targets both wild-type and variant TTR messenger RNA in the hepatocyte for degradation, thereby rapidly knocking

down circulating levels of TTR protein^{6,7}. In HELIOS-B, vutrisiran significantly decreased rates of cardiovascular events and all-cause death among patients with ATTR-CM compared with placebo, and preserved functional capacity and quality of life⁶. In this analysis, we examined the effects of vutrisiran on echocardiographic measures of cardiac structure and function in patients with ATTR-CM who took part in the HELIOS-B trial.

Results

Baseline characteristics

Among the 655 patients enrolled in HELIOS-B, 326 were randomized to vutrisiran and 329 to placebo. Baseline characteristics have been previously reported and were well balanced between treatment groups, with the exception of higher N-terminal pro-B-type natriuretic peptide (NT-proBNP) and troponin I levels in the vutrisiran group than the placebo group in the monotherapy population⁶. Median (interquartile range (IQR)) age was 77 years (45–85), 93% were male, 88% had wild-type ATTR-CM, 91% New York Heart Association (NYHA) functional class ≤II and 67% National Amyloidosis Centre (NAC) stage I. Among the 76 (12%) patients with variant ATTR-CM, the most common variant was V122I. Median (IQR) NT-proBNP level was 1,920 ng l⁻¹ (1,100–3,206). Overall, 40% of patients in the vutrisiran group and 39% of patients in the placebo group were using tafamidis at baseline (tafamidis subgroup); the remaining 395 patients constituted the vutrisiran monotherapy population, in whom tafamidis was initiated in 22% of patients in the vutrisiran group and 21% of patients in the placebo group after a median (IQR) follow-up of 17.6 months (12.2–28.1) (Extended Data Table 1).

Table 1 presents baseline echocardiographic characteristics, which were similar between treatment groups. Left ventricular (LV) wall thickness and LV mass index were increased, and the LV cavity was nondilated. Diastolic parameters were indicative of diastolic dysfunction, as suggested by low early diastolic mitral annular tissue velocities (e'), left atrial (LA) enlargement, and elevated early to late diastolic transmitral flow velocities (E/A) and E/e' ratios. Despite preserved LVEF, absolute GLS and LV stroke volume were reduced. Right ventricular (RV) free wall thickness was increased and RV function, as assessed by tricuspid annular systolic myocardial velocity (RV S'), was mildly impaired. Baseline echocardiographic parameters according to treatment assignment in the vutrisiran monotherapy population and in the baseline tafamidis subgroup are shown in Table 1.

Effect of vutrisiran on echocardiographic parameters

In the placebo group, mean LV wall thickness and LV mass index increased from baseline to month 30. Treatment with vutrisiran attenuated the increases (least squares (LS) mean difference mean LV wall thickness: -0.4 mm; 95% confidence interval (CI): -0.8 , 0.0 ; $P = 0.03$, LV mass index: -10.6 g m⁻²; 95% CI: -18.0 , -3.3 ; $P = 0.01$) (Fig. 1a,b and Table 2). Vutrisiran significantly improved diastolic function across numerous parameters including e' velocity, E/A and E/e' ratios (lateral e' velocity: 5.5 mm s⁻¹; 95% CI: 2.4 , 8.5 ; $P < 0.01$; E/A ratio: -0.3 ; 95% CI: -0.6 , 0.0 ; $P = 0.04$; average E/e' ratio: -2.0 ; 95% CI: -2.9 , -1.2 ; $P < 0.01$) (Fig. 1c,d). The LA enlarged during follow-up in both treatment groups and vutrisiran did not significantly alter LA size compared with placebo (LA volume index: -0.7 ml m⁻²; 95% CI: -2.3 , 0.9 ; $P = 0.37$). LV systolic function, as measured by LVEF, absolute GLS and LV stroke volume, worsened in both treatment groups during follow-up, and vutrisiran significantly and consistently attenuated the decline in these measures of LV systolic function compared with placebo (LVEF: 2.0% ; 95% CI: 0.3 , 3.7 ; $P = 0.02$; absolute GLS: 1.2% ; 95% CI: 0.7 , 1.7 ; $P < 0.01$; LV stroke volume: 4.1 ml; 95% CI: 1.7 , 6.4 ; $P = 0.01$) (Fig. 1e–g). Vutrisiran also attenuated the decline in RV S' at 30 months (7.0 mm s⁻¹; 95% CI: 2.8 , 11.2 ; $P < 0.01$) (Fig. 1h). These treatment effects were consistent in sensitivity analyses in which missing data were imputed (Extended Data Table 2).

In the vutrisiran monotherapy population, the treatment effects of vutrisiran, compared with placebo, on LV structure and diastolic

and systolic function were similar or greater in magnitude as was seen in the overall population (Fig. 1 and Table 2). In the baseline tafamidis subgroup, the treatment effect of vutrisiran versus placebo was broadly consistent although analyses were underpowered to evaluate treatment differences in this subgroup (Table 3).

Both in the overall population and in the vutrisiran monotherapy population, the effects of vutrisiran on key echocardiographic parameters including mean LV wall thickness, LV mass index, E/A and E/e' ratios, GLS, LVEF and LV stroke volume were consistent across prespecified subgroups (Supplementary Figs. 1–7).

Temporal changes according to treatment assignment

In both treatment groups, mean LV wall thickness and LV mass index increased steadily during follow-up, with attenuation in this increase in the vutrisiran arm that was apparent by month 30 (Fig. 2a,b and Extended Data Figs. 1 and 2). While E/e' rose (worsened) in the placebo group during follow-up, it declined (improved) in the vutrisiran group, driven largely by an increase in e' velocity (Fig. 2c,d and Extended Data Figs. 3 and 4). Significant between-group differences in E/e' were observed as early as 12 months. Between-group differences in LV systolic function were observed by 18 months with vutrisiran attenuating the progressive worsening in LVEF, GLS and LV stroke volume observed in the placebo group (Fig. 2e–g and Extended Data Figs. 5–7). Similarly, vutrisiran attenuated the decline in RV S' with significant between-group differences observed at 18 months (Fig. 2h and Extended Data Fig. 8).

Discussion

In this prespecified analysis of the HELIOS-B trial, vutrisiran positively affected echocardiographic measures of cardiac structure and function, improved diastolic function, and significantly attenuated declines in LV systolic function and increases in LV wall thickness and LV mass index over 30 months. The magnitude of the treatment effect of vutrisiran compared with placebo was similar or greater in the vutrisiran monotherapy population. Significant improvement in diastolic function with vutrisiran emerged early, followed by significant favorable effects on LV systolic function and cardiac structure.

Owing to advances in non-invasive diagnostic imaging modalities, increased awareness of ATTR-CM as a cause of HF and growing use of disease-modifying therapies, current patients with ATTR-CM are often identified earlier and have less advanced disease at the time of diagnosis compared with historic cohorts⁸. Concordant with this temporal trend, all-cause mortality was substantially lower in HELIOS-B as compared with previous randomized trials of patients with ATTR-CM including ATTR-ACT and ATTRIBUTE-CM^{6,9,10}. While HELIOS-B enrolled patients with a wide range of disease severity, on average, patients also had a better functional status and less advanced LV systolic dysfunction compared with patients enrolled in ATTR-ACT (mean LVEF 56% versus 49%; global longitudinal strain -14% versus -9% ; LV stroke volume 52 ml versus 46 ml). These observations mirror findings from the NAC, where patients with ATTR-CM exhibited less pathologic remodeling, less biventricular systolic dysfunction and lower mortality compared with patients referred during earlier periods⁹. The clinical and echocardiographic characteristics of patients enrolled in HELIOS-B were, however, representative of those of contemporary patients with ATTR-CM. Most patients had wild-type ATTR-CM, with preserved LVEF but mildly reduced absolute GLS and stroke volume, mild LA enlargement, diastolic dysfunction and moderately increased LV wall thickness⁸.

ATTR-CM is a progressive disease, characterized on echocardiography by gradual increases in LV wall thickness and progressive deterioration of LV systolic and diastolic function as amyloid infiltrates the myocardium, distorts normal tissue architecture, increases chamber stiffness and causes myocyte injury^{3,5}. In HELIOS-B, vutrisiran attenuated these increases in LV wall thickness and LV mass index

Table 1 | Baseline echocardiographic parameters according to treatment assignment

Echocardiographic parameter	Overall population			Monotherapy population		
	<i>n</i>	Placebo (<i>n</i> =328)	Vutrisiran (<i>n</i> =326)	<i>n</i>	Placebo (<i>n</i> =199)	Vutrisiran (<i>n</i> =196)
LV structure						
Mean LV wall thickness (mm)	645	18.2 (2.7)	18.2 (2.6)	388	18.3 (2.9)	18.2 (2.7)
LVEDD (mm)	642	42.7 (5.9)	42.6 (5.8)	387	42.7 (5.5)	42.9 (5.6)
LVEDV (ml)	630	95.6 (29.0)	93.9 (25.9)	377	92.8 (25.0)	91.1 (25.2)
LVESD (mm)	576	33.7 (6.1)	33.7 (5.7)	343	33.5 (5.8)	33.3 (6.1)
LVESV (ml)	627	43.4 (23.2)	43.0 (21.0)	374	42.3 (20.4)	42.4 (20.2)
LV mass index (g m ⁻²)	637	180.8 (46.1)	182.1 (44.2)	382	185.7 (49.5)	186.7 (46.8)
LV systolic function						
LVEF (%)	627	55.9 (12.4)	55.6 (12.7)	374	55.7 (12.1)	54.8 (12.6)
Absolute GLS (%)	652	14.0 (3.5)	14.0 (3.5)	393	14.3 (3.5)	14.0 (3.4)
Stroke volume (ml)	616	53.8 (19.0)	50.7 (16.3)	373	55.8 (19.6)	51.2 (16.8)
TDI lateral <i>s'</i> (mms ⁻¹)	621	49.4 (16.1)	49.5 (15.8)	375	49.8 (15.7)	50.1 (16.7)
TDI septal <i>s'</i> (mms ⁻¹)	630	42.0 (11.8)	41.5 (12.6)	383	42.3 (12.1)	41.6 (13.1)
LV diastolic function						
<i>E/A</i> ratio	353	1.9 (1.0)	2.1 (1.1)	202	1.9 (1.0)	2.1 (1.1)
<i>E</i> wave (mms ⁻¹)	644	806.7 (199.3)	804.0 (203.4)	387	802.5 (184.1)	814.1 (212.3)
<i>A</i> wave (mms ⁻¹)	354	489.0 (229.2)	461.4 (226.3)	202	512.5 (235.6)	488.8 (248.5)
Deceleration time (ms)	627	211.8 (55.5)	214.3 (59.0)	375	203.4 (50.7)	209.7 (57.3)
TDI lateral <i>e'</i> (mms ⁻¹)	627	58.5 (20.5)	61.4 (22.6)	380	58.3 (19.8)	61.2 (22.6)
TDI septal <i>e'</i> (mms ⁻¹)	632	41.3 (12.1)	42.9 (14.3)	383	42.1 (12.7)	42.6 (14.0)
<i>E/e'</i> lateral	620	15.3 (6.3)	14.8 (6.7)	321	15.3 (5.7)	15.1 (7.1)
<i>E/e'</i> septal	625	21.1 (8.3)	20.5 (7.9)	377	20.5 (6.9)	20.9 (8.0)
<i>E/e'</i> average	612	18.2 (6.1)	17.7 (6.6)	367	18.0 (5.6)	18.0 (6.8)
LA size and function						
LA diameter (mm)	632	41.3 (4.8)	41.7 (5.8)	378	40.9 (4.5)	42.0 (6.1)
LA volume index (ml m ⁻²)	638	38.4 (10.4)	39.0 (10.3)	383	38.7 (9.7)	40.4 (10.4)
TDI lateral <i>a'</i> (mms ⁻¹)	403	42.6 (20.5)	43.2 (22.3)	242	42.7 (19.8)	45.5 (24.1)
TDI septal <i>a'</i> (mms ⁻¹)	345	40.8 (19.1)	39.8 (18.2)	203	42.0 (19.1)	42.1 (19.7)
RV and pulmonary pressure						
RV free wall thickness (mm)	457	8.3 (1.9)	8.1 (1.8)	283	8.6 (2.0)	8.4 (1.9)
RV end-diastolic area (cm ²)	558	22.3 (6.1)	21.6 (5.1)	325	21.4 (5.1)	21.6 (5.1)
RV end-systolic area (cm ²)	554	13.8 (4.5)	13.0 (3.6)	322	13.4 (3.6)	13.1 (3.7)
RV <i>S'</i> (mms ⁻¹)	625	93.5 (27.2)	94.0 (26.6)	374	94.8 (28.1)	93.4 (28.1)
TR velocity (ms ⁻¹)	535	2.5 (0.4)	2.6 (0.5)	308	2.5 (0.4)	2.5 (0.5)
Maximal IVC diameter (mm)	508	20.2 (5.5)	20.4 (5.3)	311	20.0 (5.2)	20.5 (5.4)

Data are descriptive and presented as mean (s.d.). *E* wave, peak early diastolic transmitral flow velocity; IVC, inferior vena cava; LVEDD, left ventricular end-diastolic dimension; LVEDV, left ventricular end-diastolic volume; LVESD, left ventricular end-systolic dimension; LVESV, left ventricular end-systolic volume; *s'*, peak systolic mitral annular tissue velocity; TDI, tissue Doppler imaging; TR, tricuspid regurgitation.

when compared with placebo over 30 months. As LV mass has been correlated with amyloid burden, attenuating increases in LV mass index likely reflects diminished amyloid deposition in the myocardium with vutrisiran therapy¹¹. The impact of TTR knockdown on LV mass has been consistently observed in prior studies of patisiran and vutrisiran in patients with variant ATTR amyloidosis with polyneuropathy, who commonly have cardiac involvement, and of patisiran in patients with ATTR-CM^{12–14}. In HELIOS-B, between-group differences in LV wall thickness and LV mass index were observed at 30 months. The rate of increase in LV wall thickness was modest as HELIOS-B enrolled predominantly patients with wild-type ATTR-CM, who are known to exhibit slower and less concentric remodeling as compared with patients with

variant ATTR-CM, particularly V122I⁵. It is therefore expected that effects on cardiac structure emerged later.

Diastolic dysfunction is a hallmark of ATTR-CM and plays a crucial role in disease pathophysiology and evolution. In the placebo group, diastolic function deteriorated during follow-up. In contrast, vutrisiran significantly improved several indices of diastolic function including *e'* velocity, *E/e'* and *E/A* ratios. These effects of vutrisiran on diastolic function emerged early with statistically significant between-group differences for *E/e'* observed as early as 12 months, earlier than expected from the time course of effects on LV structure. While vutrisiran had beneficial effects on multiple measures of diastolic function, the effect on LA size compared with placebo was not statistically significant. Extensive

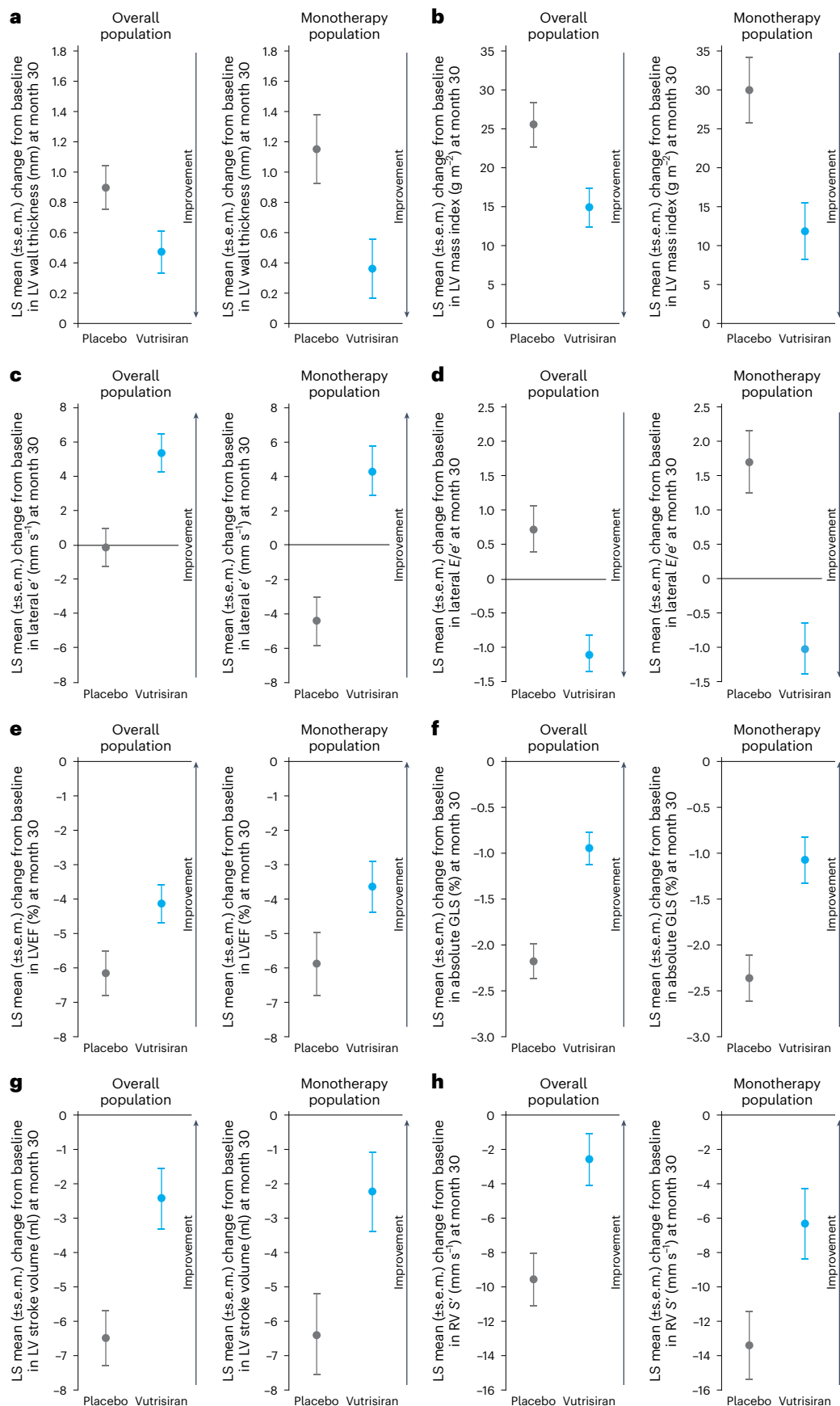


Fig. 1 | Changes in echocardiographic parameters from baseline to month 30 in the vutrisiran versus placebo groups in the overall and monotherapy populations. a–h, LS mean changes in mean LV wall thickness (a), LV mass index (b), lateral e' velocity (c), lateral E/e' (d), LVEF (e), absolute GLS (f), LV stroke

volume (g) and RV S' (h) from baseline to month 30 for vutrisiran versus placebo for the overall and monotherapy populations. Dots represent the LS mean change from baseline to month 30 and the error bars represent the s.e.m. Sample size for each echocardiographic parameter can be found in Table 2.

Table 2 | Changes in echocardiographic parameters from baseline and treatment differences at month 30

Echocardiographic parameter	Overall population					Monotherapy population				
	n	Placebo (n=328)	Vutrisiran (n=326)	Placebo-corrected treatment difference at month 30 (95% CI)	P value	n	Placebo (n=199)	Vutrisiran (n=196)	Placebo-corrected treatment difference at month 30 (95% CI)	P value
LV structure										
Mean LV wall thickness (mm)	455	0.9 (0.1)	0.5 (0.1)	−0.4 (−0.8, 0.0)	0.03	247	1.1 (0.2)	0.4 (0.2)	−0.8 (−1.4, −0.2)	0.01
LVEDD (mm)	442	0.7 (0.3)	0.6 (0.2)	−0.1 (−0.8, 0.6)	0.84	240	0.0 (0.3)	0.3 (0.3)	0.3 (−0.6, 1.2)	0.51
LVEDV (ml)	445	0.4 (1.2)	−1.7 (1.0)	−2.1 (−5.1, 1.0)	0.18	239	0.8 (1.6)	−1.4 (1.4)	−2.2 (−6.2, 1.9)	0.29
LVESD (mm)	375	1.0 (0.3)	−0.2 (0.3)	−1.2 (−2.1, −0.4)	<0.01	195	0.8 (0.4)	−0.2 (0.3)	−1.0 (−2.0, 0.1)	0.07
LVESV (ml)	434	5.9 (0.9)	3.0 (0.8)	−2.9 (−5.3, −0.6)	0.01	232	5.3 (1.2)	2.4 (1.0)	−2.9 (−6.0, 0.1)	0.06
LV mass index (g m ^{−2})	434	25.4 (2.8)	14.8 (2.5)	−10.6 (−18.0, −3.3)	<0.01	234	29.8 (4.2)	11.8 (3.7)	−18.0 (−28.9, −7.1)	<0.01
LV systolic function										
LVEF (%)	434	−6.2 (0.7)	−4.1 (0.6)	2.0 (0.3, 3.7)	0.02	232	−5.9 (0.9)	−3.6 (0.8)	2.3 (−0.1, 4.6)	0.06
Absolute GLS (%)	471	−2.2 (0.2)	−1.0 (0.2)	1.2 (0.7, 1.7)	<0.01	257	−2.4 (0.3)	−1.1 (0.3)	1.3 (0.6, 2.0)	<0.01
Stroke volume (ml)	427	−6.5 (0.8)	−2.4 (0.9)	4.1 (1.7, 6.4)	<0.01	237	−6.4 (1.2)	−2.2 (1.2)	4.2 (0.9, 7.4)	0.01
TDI lateral s' (mms ^{−1})	426	−1.1 (0.9)	3.5 (0.9)	4.6 (2.1, 7.2)	<0.01	233	−4.0 (1.1)	2.1 (1.2)	6.1 (2.9, 9.3)	<0.01
TDI septal s' (mms ^{−1})	432	−3.0 (0.7)	0.8 (0.7)	3.8 (1.9, 5.6)	<0.01	240	−6.0 (0.8)	−0.6 (0.9)	5.4 (3.0, 7.9)	<0.01
LV diastolic function										
E/A ratio	175	0.4 (0.1)	0.1 (0.1)	−0.3 (−0.6, 0.0)	0.04	91	0.6 (0.2)	0.1 (0.1)	−0.4 (−0.8, 0.0)	0.05
E wave (mms ^{−1})	450	24.3 (10.6)	18.4 (9.3)	−5.8 (−33.5, 21.9)	0.68	245	11.7 (13.7)	5.5 (12.1)	−6.1 (−42.1, 29.8)	0.74
A wave (mms ^{−1})	178	−62.2 (18.4)	−6.1 (15.3)	56.1 (8.9, 103.2)	0.02	91	−86.9 (30.0)	−9.5 (20.1)	77.3 (5.4, 149.2)	0.04
Deceleration time (ms)	419	−22.7 (2.9)	−19.9 (2.9)	2.77 (−5.4, 10.9)	0.50	227	−18.0 (3.9)	−6.9 (4.3)	11.1 (−0.3, 22.5)	0.06
TDI lateral e' (mms ^{−1})	438	−0.2 (1.1)	5.3 (1.1)	5.5 (2.4, 8.5)	<0.01	244	−4.5 (1.4)	4.3 (1.4)	8.7 (4.8, 12.6)	<0.01
TDI septal e' (mms ^{−1})	433	−1.6 (0.7)	2.2 (0.7)	3.8 (1.8, 5.8)	<0.01	241	−5.0 (1.0)	0.1 (0.9)	5.2 (2.6, 7.7)	<0.01
E/e' lateral	419	0.7 (0.3)	−1.08 (0.3)	−1.8 (−2.7, −1.0)	<0.0001	231	1.7 (0.5)	−1.0 (0.4)	−2.7 (−3.9, −1.6)	<0.0001
E/e' septal	415	1.7 (0.4)	−0.6 (0.4)	−2.3 (−3.4, −1.2)	<0.0001	229	3.2 (0.6)	−0.0 (0.5)	−3.2 (−4.7, −1.7)	<0.0001
E/e' average	402	1.2 (0.3)	−0.8 (0.3)	−2.0 (−2.9, −1.2)	<0.01	219	2.3 (0.5)	−0.6 (0.4)	−2.9 (−4.1, −1.7)	<0.01
LA size and function										
LA diameter (mm)	422	0.7 (0.3)	0.6 (0.3)	−0.1 (−1.0, 0.7)	0.72	224	0.5 (0.4)	0.8 (0.4)	0.2 (−1.0, 1.4)	0.73
LA volume index (ml m ^{−2})	457	5.7 (0.6)	5.0 (0.5)	−0.7 (−2.3, 0.9)	0.37	248	5.2 (0.8)	4.7 (0.8)	−0.5 (−2.6, 1.7)	0.67
TDI lateral a' (mms ^{−1})	226	−4.9 (1.5)	−0.9 (1.4)	4.0 (−0.1, 8.0)	0.05	128	−9.7 (2.1)	−4.1 (1.8)	5.6 (0.2, 11.1)	0.04
TDI septal a' (mms ^{−1})	189	−6.4 (1.5)	−3.4 (1.3)	3.0 (−0.8, 6.9)	0.12	107	−11.2 (2.2)	−3.7 (1.7)	7.5 (2.1, 13.0)	0.01
RV and pulmonary pressure										
RV free wall thickness (mm)	255	1.7 (0.0)	1.4 (0.0)	−0.4 (−0.8, 0.0)	0.07	142	1.5 (0.3)	1.0 (0.3)	−0.5 (−1.1, 0.1)	0.10
RV end-diastolic area (cm ²)	337	0.1 (0.3)	−0.4 (0.4)	−0.5 (−1.5, 0.4)	0.28	178	0.6 (0.4)	−0.1 (0.5)	−0.7 (−2.0, 0.6)	0.30
RV end-systolic area (cm ²)	319	1.8 (0.3)	1.6 (0.3)	−0.2 (−0.9, 0.6)	0.65	169	1.9 (0.4)	1.4 (0.4)	−0.6 (−1.6, 0.4)	0.25
RV S' (mms ^{−1})	408	−9.6 (1.5)	−2.6 (1.5)	7.0 (2.8, 11.2)	<0.01	226	−13.4 (2.0)	−6.3 (2.0)	7.1 (1.5, 12.7)	0.01
TR velocity (ms ^{−1})	334	−0.1 (0.0)	−0.2 (0.0)	0.0 (−0.1, 0.1)	0.60	168	−0.1 (0.0)	−0.1 (0.1)	0.0 (−0.1, 0.1)	0.89
Maximal IVC diameter (mm)	325	1.5 (0.3)	0.2 (0.3)	−1.3 (−2.2, −0.3)	0.01	171	2.1 (0.4)	0.6 (0.4)	−1.6 (−2.8, −0.3)	0.01

Results are reported as the LS mean difference (standard error of the mean (s.e.m.)) derived from repeated measures models with baseline as a covariate and fixed-effect terms including the treatment group, visit, treatment-by-visit interaction, type of ATTR amyloidosis and age group. The overall population also included baseline tafamidis use and treatment-by-baseline tafamidis use interaction as fixed-effect terms.

amyloid infiltration of the atria, as shown by histology and cardiac magnetic resonance imaging, causes poor compliance and impaired LA contractile function^{15–17}. Poor compliance limits atrial remodeling in response to rising ventricular filling pressures. Interestingly, peak late diastolic mitral annular tissue velocity (α') and peak late diastolic transmitral flow velocity (A wave) decreased in the placebo group but remained stable in the vutrisiran group during follow-up. Whether this represents preservation of LA contractile function, favorable effects on

LV compliance or a combination of both deserves further exploration with more sensitive measures of LA function.

LV systolic function, an important and independent predictor of mortality in patients in ATTR-CM, deteriorated during follow-up. The rate of decline in LVEF and absolute GLS in the placebo group was comparable to that observed in the placebo arm of ATTR-ACT and in retrospective cohort studies^{5,9,18}. Compared with placebo, vutrisiran attenuated declines in LV systolic function across multiple indices

Table 3 | Baseline echocardiographic parameters and changes from baseline to month 30 in the baseline tafamidis subgroup

Echocardiographic parameter	Baseline			LS mean change at month 30		Placebo-corrected treatment difference (95% CI)
	N	Placebo (n=129)	Vutrisiran (n=130)	Placebo (n=129)	Vutrisiran (n=130)	
LV structure						
Mean LV wall thickness (mm)	257	18.0 (2.4)	18.2 (2.6)	0.5 (0.2)	0.6 (0.2)	0.1 (−0.1, 0.6)
LVEDD (mm)	255	42.8 (6.5)	42.3 (6.1)	1.7 (0.4)	1.1 (0.4)	−0.6 (−1.7, 0.5)
LVEDV (ml)	253	99.9 (33.9)	98.0 (26.4)	0.08 (1.7)	−2.0 (1.5)	−2.1 (−6.6, 2.4)
LVESD (mm)	233	34.0 (6.5)	34.3 (5.1)	1.3 (0.5)	−0.3 (0.4)	−1.5 (−2.8, −0.3)
LVESV (ml)	253	45.1 (26.9)	43.8 (22.2)	6.9 (1.4)	3.9 (1.1)	−3.0 (−6.5, 0.5)
LV mass index (g m ^{−2})	255	173.2 (39.2)	175.3 (39.3)	19.9 (3.6)	18.6 (3.2)	−1.3 (−10.8, 8.3)
LV systolic function						
LVEF (%)	253	56.3 (12.8)	56.9 (12.8)	−6.4 (0.9)	−4.8 (0.8)	1.5 (−0.9, 4.0)
Absolute GLS (%)	259	13.5 (3.4)	13.9 (3.5)	−1.9 (0.3)	−0.8 (0.2)	1.1 (0.4, 1.8)
Stroke volume (ml)	243	50.7 (17.8)	50.0 (15.5)	−6.3 (1.1)	−2.6 (1.3)	3.7 (0.4, 7.1)
TDI lateral s' (mms ^{−1})	246	48.9 (16.8)	48.7 (14.5)	2.9 (1.4)	5.0 (1.5)	2.2 (−1.9, 6.3)
TDI septal s' (mms ^{−1})	247	41.6 (11.1)	41.4 (11.7)	1.1 (1.0)	2.6 (1.0)	1.5 (−1.3, 4.3)
LV diastolic function						
E/A ratio	151	2.1 (1.1)	2.2 (1.1)	0.2 (0.1)	0.1 (0.1)	−0.1 (−0.5, 0.3)
E wave (mms ^{−1})	257	813.0 (221.1)	789.0 (189.3)	38.4 (16.8)	39.0 (14.4)	0.5 (−43.2, 44.2)
A wave (mms ^{−1})	152	457.0 (217.8)	425.6 (189.3)	−18.9 (21.6)	−3.0 (23.6)	15.9 (−47.5, 79.3)
Deceleration time (ms)	252	224.3 (60.0)	221.2 (61.0)	−28.3 (4.5)	−36.7 (3.8)	−8.4 (−20.0, 3.2)
TDI lateral e' (mms ^{−1})	247	58.9 (21.5)	61.7 (22.7)	5.9 (1.7)	6.6 (1.7)	0.7 (−4.1, 5.5)
TDI septal e' (mms ^{−1})	249	39.9 (11.2)	43.4 (14.8)	3.1 (1.1)	5.0 (1.2)	1.9 (−1.3, 5.0)
E/e' lateral	246	15.4 (7.2)	14.4 (6.1)	−0.6 (0.5)	−1.1 (0.4)	−0.5 (−1.7, 0.7)
E/e' septal	248	21.9 (10.1)	20.0 (7.8)	−0.2 (0.6)	−1.3 (0.5)	−1.1 (−2.6, 0.5)
E/e' average	245	18.4 (6.8)	17.2 (6.3)	−0.4 (0.5)	−1.2 (0.4)	−0.8 (−1.9, 0.4)
LA size and function						
LA diameter (mm)	254	41.9 (5.3)	41.2 (5.4)	0.9 (0.4)	0.3 (0.4)	−0.6 (−1.7, 0.6)
LA volume index (mlm ^{−2})	255	38.0 (11.5)	36.9 (9.8)	6.2 (0.9)	5.2 (0.7)	−1.0 (−3.3, 1.3)
TDI lateral a' (mms ^{−1})	161	42.5 (21.7)	39.7 (19.0)	1.8 (2.0)	3.0 (2.2)	1.1 (−4.7, 7.0)
TDI septal a' (mms ^{−1})	142	39.1 (19.2)	36.6 (15.4)	0.1 (2.0)	−2.6 (1.9)	−2.6 (−8.2, 3.0)
RV and pulmonary pressure						
RV free wall thickness (mm)	174	7.7 (0.2)	7.5 (0.2)	1.9 (0.2)	1.7 (0.2)	−0.3 (−0.9, 0.4)
RV end-diastolic area (cm²)	233	23.5 (7.1)	21.6 (5.1)	−0.4 (0.5)	−0.9 (0.5)	−0.5 (−1.9, 1.0)
RV end-systolic area (cm²)	232	14.3 (5.4)	12.7 (3.6)	1.6 (0.4)	1.8 (0.4)	0.2 (−0.9, 1.3)
RV S' (mms ^{−1})	251	91.4 (25.6)	95.0 (24.4)	−4.0 (2.4)	2.8 (2.3)	6.8 (0.3, 13.3)
TR velocity (ms ^{−1})	227	2.6 (0.4)	2.6 (0.5)	−0.2 (0.0)	−0.2 (0.0)	−0.0 (−0.1, 0.1)
Maximal IVC diameter (mm)	197	20.4 (5.9)	20.2 (5.1)	0.6 (0.5)	−0.2 (0.5)	−0.8 (−2.3, 0.7)

Results are reported as the LS mean difference (s.e.m.) derived from repeated measures models with baseline as a covariate and fixed-effect terms including the treatment group, visit, treatment-by-visit interaction, type of ATTR amyloidosis and age group. The overall population also included baseline tafamidis use and treatment-by-baseline tafamidis use interaction as fixed-effect terms.

with significant between-group differences observed as early as 18 months. The magnitude of the treatment effect of vutrisiran on measures of LV systolic function including LVEF, GLS and LV stroke volume was comparable with that of tafamidis in ATTR-ACT although comparisons are difficult to draw between the two trials owing to differences in patient characteristics, disease severity and background treatment¹⁸. Notably, tafamidis attenuated worsening in the E/e' ratio in ATTR-ACT whereas vutrisiran improved the E/e' ratio in HELIOS-B compared with placebo¹⁸. As measures of LV systolic function including GLS have been correlated with amyloid burden, inhibiting further

amyloid deposition in the myocardium may underlie the favorable effects of vutrisiran on LV systolic function¹⁹. The treatment effects of vutrisiran on systolic and diastolic function also complement its favorable effects on NT-proBNP, a marker of ventricular wall stress and important prognostic marker in ATTR-CM, and cardiac troponin, a marker of myocardial injury⁶. The effects of vutrisiran on cardiac structure and function were similar or larger in magnitude in the vutrisiran monotherapy population.

The beneficial effects of vutrisiran on echocardiographic measures of cardiac structure and function are clinically meaningful as

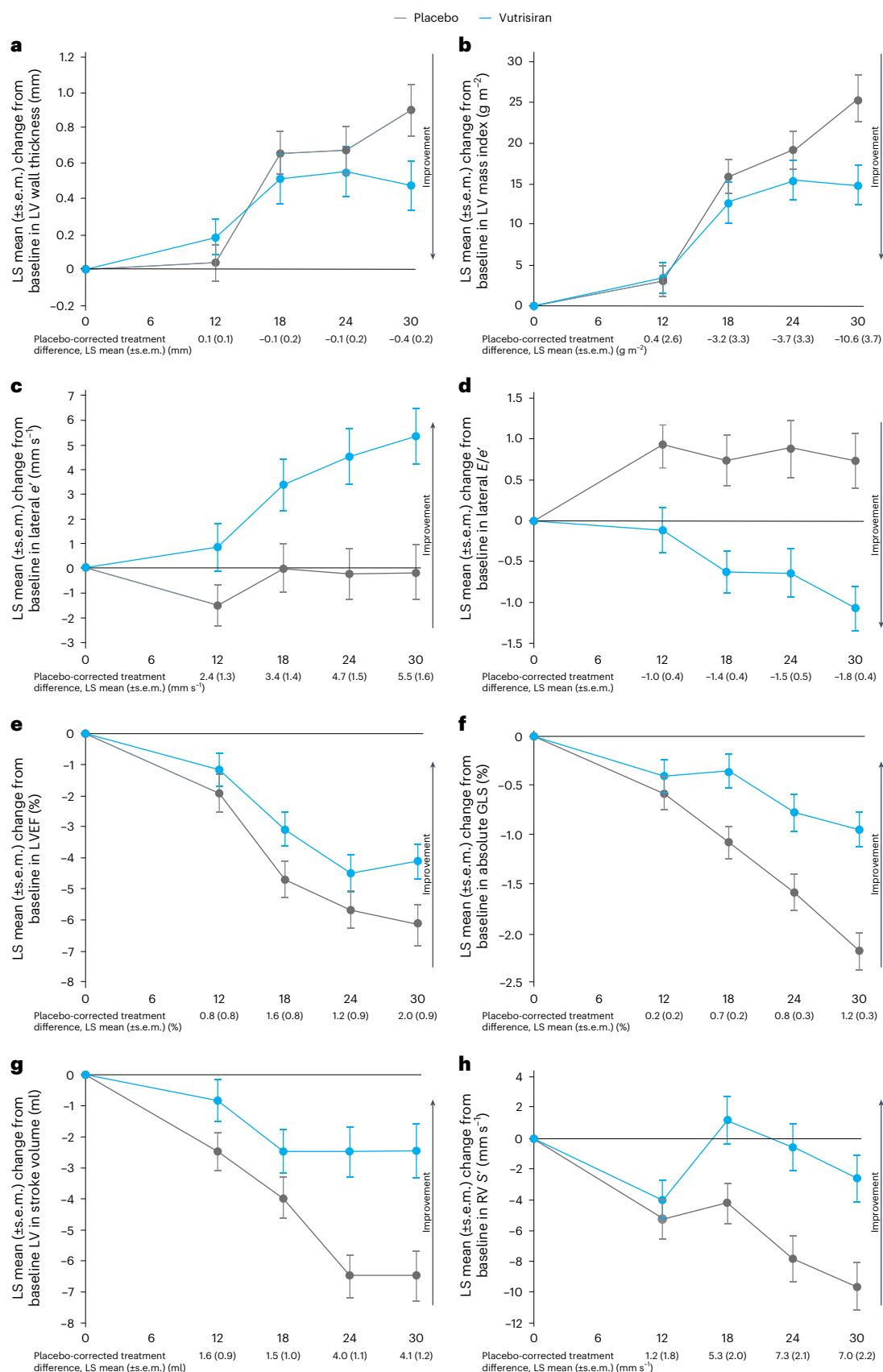


Fig. 2 | Effect of vutrisiran compared with placebo on echocardiographic parameters over time in the overall population. a–h, LS mean changes over time in mean LV wall thickness (a), LV mass index (b), lateral e' velocity (c), lateral

E/e' (d), LVEF (e), absolute GLS (f), LV stroke volume (g) and RV S' (h) according to treatment assignment in the overall population. Error bars represent the s.e.m. Sample size for each echocardiographic parameter can be found in Table 2.

they were observed despite substantial background use of tafamidis (40% at baseline with an additional 22% drop in in the monotherapy population during follow-up)⁶ (Extended Data Table 1). The echocardiographic parameters positively affected by vutrisiran including E/e' , GLS, LVEF and stroke volume are known to be prognostically important in patients with ATTR-CM^{20,21}. Differences of the magnitude observed with vutrisiran in HELIOS-B in these parameters have been shown to be independently associated with mortality. Furthermore, declines in LV stroke volume index over 12 months as well as worsening severity of mitral and tricuspid regurgitation in untreated patients with ATTR-CM have been independently associated with a higher risk of all-cause mortality⁵. These findings suggest that declines in the effective forward stroke volume as the final common pathway in ATTR-CM portend a worse prognosis, as would be expected in a patient population with restrictive physiology. The beneficial effects of vutrisiran on cardiac function, including on LV stroke volume, may therefore contribute to improved outcomes. Furthermore, the time course of beneficial effects on LV structure and function provides a mechanistic explanation for the impact soon after vutrisiran treatment initiation on reducing the risk of worsening heart failure²². The findings support early use of vutrisiran in patients with ATTR-CM regardless of background therapy.

The present findings should be interpreted in the context of study limitations. Although tafamidis was used in 40% of patients at baseline, the study was not powered to estimate treatment effects in the tafamidis subgroup. Racial diversity and enrollment of women were limited in HELIOS-B, reflecting the reported demographic characteristics of patients with ATTR-CM^{2,8}. Consistent with the prevalence of wild-type ATTR-CM and male predominance, a lower proportion of patients with variant ATTR-CM and women were enrolled, which likewise limited the power to estimate treatment effects in these subgroups⁸. Information on severity of valvular disease was not collected.

In conclusion, in this current population of patients with ATTR-CM, vutrisiran had beneficial impact across all domains of cardiac structure, systolic and diastolic function consistent with its beneficial effects on clinical outcomes, biomarkers and health status. The beneficial effects of vutrisiran on cardiac structure and function likely underlie the reduced risk of cardiovascular events and all-cause mortality, as well as outpatient worsening HF. These favorable effects on cardiac structure and both systolic and diastolic function, despite extensive use of background therapy, further support its use as a disease-modifying therapy for patients newly diagnosed with ATTR-CM and those progressing on stabilizing therapies.

Online content

Any methods, additional references, Nature Portfolio reporting summaries, source data, extended data, supplementary information, acknowledgements, peer review information; details of author contributions and competing interests; and statements of data and code availability are available at <https://doi.org/10.1038/s41591-025-03851-z>.

References

- Ruberg, F. L., Grogan, M., Hanna, M., Kelly, J. W. & Maurer, M. S. Transthyretin amyloid cardiomyopathy: JACC state-of-the-art review. *J. Am. Coll. Cardiol.* **73**, 2872–2891 (2019).
- Ruberg, F. L. & Maurer, M. S. Cardiac amyloidosis due to transthyretin protein: a review. *JAMA* **331**, 778–791 (2024).
- Garcia-Pavia, P. et al. Expert consensus on the monitoring of transthyretin amyloid cardiomyopathy. *Eur. J. Heart Fail.* **23**, 895–905 (2021).
- Dorbala, S. et al. ASNC/AHA/ASE/EANM/HFSA/ISA/SCMR/SNMMI expert consensus recommendations for multimodality imaging in cardiac amyloidosis: part 2 of 2—diagnostic criteria and appropriate utilization. *Circ.: Cardiovasc. Imaging* **14**, e000030 (2021).
- Chacko, L. et al. Progression of echocardiographic parameters and prognosis in transthyretin cardiac amyloidosis. *Eur. J. Heart Fail.* **24**, 1700–1712 (2022).
- Fontana, M. et al. Vutrisiran in patients with transthyretin amyloidosis with cardiomyopathy. *N. Engl. J. Med.* **392**, 33–44 (2025).
- Adams, D. et al. Efficacy and safety of vutrisiran for patients with hereditary transthyretin-mediated amyloidosis with polyneuropathy: a randomized clinical trial. *Amyloid* **30**, 1–9 (2023).
- Ioannou, A. et al. Impact of earlier diagnosis in cardiac ATTR amyloidosis over the course of 20 years. *Circulation* **146**, 1657–1670 (2022).
- Maurer, M. S. et al. Tafamidis treatment for patients with transthyretin amyloid cardiomyopathy. *N. Engl. J. Med.* **379**, 1007–1016 (2018).
- Gillmore, J. D. et al. Efficacy and safety of acoramidis in transthyretin amyloid cardiomyopathy. *N. Engl. J. Med.* **390**, 132–142 (2024).
- Knight, D. S. et al. Cardiac structural and functional consequences of amyloid deposition by cardiac magnetic resonance and echocardiography and their prognostic roles. *JACC: Cardiovasc. Imaging* **12**, 823–833 (2019).
- Solomon, S. D. et al. Effects of patisiran, an RNA interference therapeutic, on cardiac parameters in patients with hereditary transthyretin-mediated amyloidosis. *Circulation* **139**, 431–443 (2019).
- Garcia-Pavia, P. et al. Impact of vutrisiran on exploratory cardiac parameters in hereditary transthyretin-mediated amyloidosis with polyneuropathy. *Eur. J. Heart* **26**, 397–410 (2024).
- Maurer, M. S. et al. Patisiran treatment in patients with transthyretin cardiac amyloidosis. *N. Engl. J. Med.* **389**, 1553–1565 (2023).
- Bandera, F. et al. Clinical importance of left atrial infiltration in cardiac transthyretin amyloidosis. *JACC: Cardiovasc. Imaging* **15**, 17–29 (2022).
- Kwong, R. Y. et al. Characterization of cardiac amyloidosis by atrial late gadolinium enhancement using contrast-enhanced cardiac magnetic resonance imaging and correlation with left atrial conduit and contractile function. *Am. J. Cardiol.* **116**, 622–629 (2015).
- Vergaro, G. et al. Atrial amyloidosis: mechanisms and clinical manifestations. *Eur. J. Heart Fail.* **24**, 2019–2028 (2022).
- Shah, S. J. et al. Effect of tafamidis on cardiac function in patients with transthyretin amyloid cardiomyopathy: a post hoc analysis of the ATTR-ACT randomized clinical trial. *JAMA Cardiol.* **9**, 25–34 (2024).
- Ternacle, J. et al. Causes and consequences of longitudinal LV dysfunction assessed by 2D strain echocardiography in cardiac amyloidosis. *JACC: Cardiovasc. Imaging* **9**, 126–138 (2016).
- Chacko, L. et al. Echocardiographic phenotype and prognosis in transthyretin cardiac amyloidosis. *Eur. Heart J.* **41**, 1439–1447 (2020).
- Quarta, C. C. et al. Left ventricular structure and function in transthyretin-related versus light-chain cardiac amyloidosis. *Circulation* **129**, 1840–1849 (2014).
- Fontana, M. et al. Outpatient worsening heart failure in patients with transthyretin amyloidosis with cardiomyopathy in the HELIOS-B trial. *J. Am. Coll. Cardiol.* **85**, 753–761 (2025).

Publisher's note Springer Nature remains neutral with regard to jurisdictional claims in published maps and institutional affiliations.

Open Access This article is licensed under a Creative Commons Attribution 4.0 International License, which permits use, sharing, adaptation, distribution and reproduction in any medium or format, as long as you give appropriate credit to the original author(s) and the source, provide a link to the Creative Commons licence, and indicate if changes were made. The images or other third party material in this article are included in the article's Creative Commons licence, unless indicated otherwise in a

credit line to the material. If material is not included in the article's Creative Commons licence and your intended use is not permitted by statutory regulation or exceeds the permitted use, you will need to obtain permission directly from the copyright holder. To view a copy of this licence, visit <http://creativecommons.org/licenses/by/4.0/>.

© The Author(s) 2025

¹Cardiovascular Division, Brigham and Women's Hospital, and Harvard Medical School, Boston, MA, USA. ²National Amyloidosis Centre, Division of Medicine, University College London, Royal Free Hospital, London, UK. ³Department of Cardiology, Toulouse University Hospital, Toulouse, France. ⁴Cardiology Unit, Cardiac Thoracic and Vascular Department, IRCCS Azienda Ospedaliero-Universitaria di Bologna, Bologna, Italy. ⁵Cardiology Department, Hospital da Senhora da Oliveira, Guimarães, Portugal. ⁶Department of Clinical Research and Epidemiology, Comprehensive Heart Failure Center, University Hospital Würzburg, Würzburg, Germany. ⁷Department of Medicine I, University Hospital Würzburg, Würzburg, Germany. ⁸Alnylam Pharmaceuticals, Cambridge, MA, USA. ✉e-mail: ssolomon@bwh.harvard.edu

Methods

HELIOS-B study design and population

The design, study protocol, statistical analysis plan and primary results of HELIOS-B have been previously reported⁶. Briefly, HELIOS-B was a double-blind, randomized, placebo-controlled trial testing the efficacy and safety of vutrisiran (25 mg administered subcutaneously every 12 weeks) versus placebo in patients with ATTR-CM. Patients aged from 18 to 85 years were eligible if they had a diagnosis of either variant or wild-type ATTR-CM established on the basis of tissue biopsy or validated scintigraphy-based diagnostic criteria with evidence of cardiac involvement (interventricular septal wall thickness >12 mm on echocardiography) and a clinical history of symptomatic HF. Additional inclusion criteria were NT-proBNP level >300 pg ml⁻¹ (>600 pg ml⁻¹ in patients with atrial fibrillation) and <8,500 pg ml⁻¹, and 6-min walk distance ≥150 m. At baseline, patients were either receiving tafamidis for ATTR-CM at the dose approved within their country or were not receiving tafamidis, with no active plan to start tafamidis during the first 12 months after randomization. Key exclusion criteria were NYHA functional class IV or NYHA III with NAC ATTR stage 3, prior use of TTR-lowering therapies and estimated glomerular filtration rate <30 ml per min per 1.73 m². A complete list of inclusion and exclusion criteria is provided in the primary publication⁶. The ethics committee at each participating site approved the study protocol (see Supplementary Appendix for full list) and patients provided written informed consent. Medidata Rave EDC v.2024.1.1 was used for case report form data collection.

Study procedures and echocardiographic methods

Certified sonographers at each site performed serial echocardiograms according to a standardized, prespecified protocol at baseline and months 12, 18, 24 and 30. Echocardiographic images were transferred to the Cardiovascular Imaging Core Laboratory (Brigham and Women's Hospital, Boston, MA, USA) for analysis. Echocardiographic measurements were performed using commercially available software (Us2.ai v.1.4 and v.2.0) by analysts blinded to clinical characteristics of study participants, treatment assignment and temporal sequence. Quantitative measurements were performed in accordance with American Society of Echocardiography guidelines^{23,24}. Laboratory-wide intra- and interobserver variability for key measures of cardiac structure and function have been previously reported^{25–27}; amongst analysts involved in this study the coefficient of variation was ≤16% and intra-class correlation ≥0.72.

Mean LV wall thickness was computed as the average of interventricular septal and posterior wall thickness in diastole and relative wall thickness as $\times 2$ posterior wall thickness in diastole/left ventricular end-diastolic diameter. LV mass was calculated from linear dimensions using Devereux's formula and indexed to body surface area. LV volumes and LVEF were derived using the modified biplane Simpson's method²³. LV stroke volume was calculated as $\pi \times (\text{LV outflow tract diameter}/2)^2 \times \text{LV outflow tract velocity time integral}$. LV GLS was measured on the Us2.ai platform²⁸. LA volume was measured from apical two- and four-chamber views at end systole. Mitral inflow (E and A wave velocities) was assessed using pulsed-wave Doppler from the apical four-chamber view and tissue velocities (e' , a' and s') were measured from the septal and lateral aspects of the mitral annulus. RV free wall thickness was measured in the subcostal views and RV function was assessed using RV S' .

Changes from baseline to month 30 in mean LV wall thickness and GLS were prespecified as exploratory endpoints in HELIOS-B. Changes in other echocardiographic parameters were not prespecified and as such are considered exploratory.

Statistical analysis

Data were summarized as frequency (percentage) for categorical variables and mean \pm s.d. or median (IQR) for continuous variables,

depending on their distribution. Changes in echocardiographic parameters from baseline to month 30 were evaluated using repeated measures models with an unstructured covariance matrix. The corresponding baseline echocardiographic parameter was included as a covariate and treatment group, visit (baseline, month 12, 18, 24 or 30), treatment-by-visit interaction, type of ATTR amyloidosis (wild-type versus variant) and age group (<75 versus ≥75 years) were included as fixed-effect terms. Changes in echocardiographic parameters were analyzed both in the overall population as well as in the vutrisiran monotherapy population, defined as patients not taking tafamidis at baseline, as previously described⁶. In the overall population, baseline tafamidis use and treatment-by-baseline tafamidis use interaction were also included as fixed-effect terms. Missing data were not imputed (the number of missing values is reported in Supplementary Table 1). A sensitivity analysis using a pattern mixture model was performed to assess the robustness of the repeated measures model results to the possible violation of the missing at random (MAR) missingness assumption. For this, patients were classified into four patterns for missing echocardiographic data during the double-blind period:

- (1) Patients who died (including those who underwent heart transplantation or LV assist device placement) before the month 30 visit: the missing change from baseline values at a postbaseline visit were imputed as sampling with replacement from the worst 10% of observed change from baseline values from all patients at the same visit and in the same treatment group and same baseline tafamidis group, capped by the worst possible change for the patient (that is 0 – baseline value).
- (2) Patients in the vutrisiran arm who were not in Pattern 1 and had missing visits within 126 days of the last dose of vutrisiran: the missing change from baseline values was considered MAR and was imputed using multiple imputation (MI) estimated from vutrisiran patients with nonmissing data collected on treatment (that is, data on visits within 126 days from last dose) in the same baseline tafamidis group. The window of 126 days was chosen as $\times 1.5$ the dosing interval of 84 days.
- (3) Patients in the vutrisiran arm who were not in Pattern 1 and had missing visits that were more than 126 days after the last dose of vutrisiran:
 - (i) If there were sufficient (that is, at least 10) retrieved dropouts at month 30 in the same baseline tafamidis group (that is, vutrisiran patients who had discontinued treatment but still had assessments that were more than 126 days after the last dose), the missing data were imputed using data from these retrieved dropouts.
 - (ii) If there were insufficient retrieved dropouts, missing change from baseline values were assumed to be missing not at random and were imputed (using data from placebo patients in the same baseline tafamidis group) using the copy reference approach.
- (4) Patients in the placebo arm who were not in Pattern 1 and had missing data for other reasons:
 - (i) If there were sufficient (that is, at least 10) retrieved dropouts at month 30 in the same baseline tafamidis group (that is, placebo patients who had discontinued study treatment but still had assessments that were more than 126 days from the last dose), the missing data were imputed using data from these retrieved dropouts.
 - (ii) If there were insufficient retrieved dropouts, missing change from baseline values were considered as MAR and imputed using MI estimated from all placebo patients in the same baseline tafamidis group.

Imputed change from baseline from any of the methods was capped by the worst possible change of the patient (0 – baseline value). For patients in Pattern (1), the imputation details were as

described above. For patients in Pattern (2) and (4ii), all missing data for the placebo arm and missing data for the vutrisiran arm during the on-treatment period (that is, assessments within 126 days of the last dose of study drug) were imputed using MI under the MAR assumption. As the pattern of missing data within patients may be nonmonotone, multiple imputation was conducted separately by treatment arm and baseline tafamidis use group using the Markov Chain Monte Carlo method. For each treatment arm or baseline tafamidis use group, the imputation model included type of ATTR amyloidosis (wild-type versus variant), NYHA class (I or II versus III), age at randomization (<75 versus ≥75 years), NT-proBNP (≤3,000 ng l⁻¹ versus >3,000 ng l⁻¹), baseline value and all postbaseline change from baseline values at protocol specified visits.

For imputation using the retrieved dropouts (Patterns (3i) and (4i)), the multiple imputation approach described in ref. 29 was adopted.

Missing values were imputed 100 times to generate 100 complete datasets using the procedures described above (via MI, copy reference or other methods described previously). An analysis of covariance (ANCOVA) model was fitted to each imputed dataset for the change from baseline in select echocardiographic parameters at month 30. The ANCOVA model included the baseline echocardiographic parameter as a covariate and treatment arm, baseline tafamidis use, treatment-by-baseline tafamidis use interaction, ATTR disease type and age group as factors. For the vutrisiran monotherapy subgroup analysis, baseline tafamidis use and treatment-by-baseline tafamidis use interaction were removed from the model.

The LS mean and standard error estimated from the ANCOVA model fit to each imputed dataset were combined by applying Rubin's rules to produce inferential results including the treatment difference in LS means and 95% CI for the treatment difference^{29–31}. Statistical significance was assessed using a two-sided alpha level of 0.05 without adjustment for multiplicity. All analyses were performed using SAS v.9.4.

Reporting summary

Further information on research design is available in the Nature Portfolio Reporting Summary linked to this article.

Data availability

Access to anonymized individual participant data that support these results will be made available 12 months after study completion and not less than 12 months after the product and indication have been approved in the United States and/or the European Union. Access to data may be declined where there is likelihood a patient could be identified or other feasibility issue, where there is a potential conflict of interest, planned business activities or an actual or potential competitive risk. Data will be provided contingent upon the approval of a research proposal and the execution of a data sharing agreement. Timeframes for data access may vary and can take up to 6 months or more. Requests for access to data can be submitted via the website www.vivli.org. Questions can also be directed to datasharing@alnylam.com.

References

- Lang, R. M. et al. Recommendations for cardiac chamber quantification by echocardiography in adults: an update from the American Society of Echocardiography and the European Association of Cardiovascular Imaging. *Eur. Heart J. Cardiovasc. Imaging* **16**, 233–270 (2015).
- Nagueh, S. F. et al. Recommendations for the evaluation of left ventricular diastolic function by echocardiography: an update from the American Society of Echocardiography and the European Association of Cardiovascular Imaging. *J. Am. Soc. Echocardiogr.* **29**, 277–314 (2016).
- Shah, A. M. et al. Cardiac structure and function in heart failure with preserved ejection fraction: baseline findings from the echocardiographic study of the Treatment of Preserved Cardiac Function Heart Failure with an Aldosterone Antagonist trial. *Circ. Heart Fail.* **7**, 104–115 (2014).
- Shah, A. M. et al. Rationale and design of a multicenter echocardiographic study to assess the relationship between cardiac structure and function and heart failure risk in a biracial cohort of community-dwelling elderly persons. *Circ.: Cardiovasc. Imaging* **7**, 173–181 (2014).
- Kraigher-Krainer, E. et al. Impaired systolic function by strain imaging in heart failure with preserved ejection fraction. *J. Am. Coll. Cardiol.* **63**, 447–456 (2014).
- Myhre, P. L. et al. External validation of a deep learning algorithm for automated echocardiographic strain measurements. *Eur. Heart J. Digit. Health* **5**, 60–68 (2024).
- Wang, S. & Hu, H. Impute the missing data using retrieved dropouts. *BMC Med. Res. Methodol.* **22**, 82 (2022).
- Rubin, D. B. *Multiple Imputation for Nonresponse in Surveys* (Wiley, 1987).
- Rubin, D. B. Multiple imputation after 18+ years. *J. Am. Stat. Assoc.* **91**, 473–489 (1996).

Acknowledgements

HELIO-B was funded by Alnylam Pharmaceuticals. Alnylam Pharmaceuticals had organizational oversight over the HELIO-B trial and was responsible for trial conduct, supervision and monitoring of the enrolling sites, data collection and storage. Data were analyzed by Alnylam Pharmaceuticals in accordance with the SAP and analytic output was independently verified by the academic group at Brigham and Women's Hospital. Graphical assistance with figures was provided by Adelphi Communications Ltd in accordance with Good Publication Practice guidelines and was funded by Alnylam Pharmaceuticals.

Author contributions

All authors made substantial contributions to the conceptualization and design of the study. S.B. and K.S.J. had full access to all the data in the study and take responsibility for the integrity of the data and the accuracy of the data analysis. K.S.J. cross verified all analytic output, which was generated by S.B. K.S.J. wrote the first draft of the manuscript. All authors contributed to data interpretation and writing of the final version of the manuscript, and were responsible for the decision to submit the manuscript for publication.

Competing interests

K.J. reports speaker fees from Alnylam Pharmaceuticals. M.F. reports consultancy/advisory boards for Alexion/Caelum Biosciences, Alnylam, AstraZeneca, Attralus, Bayer, BridgeBio/Eidos, Cardior, Intellia Therapeutics, Ionis Pharmaceuticals, Janssen Pharmaceuticals, Lexeo Therapeutics, Mycardium, Novo Nordisk, Pfizer and Prothena; research grants from Alnylam, AstraZeneca, BridgeBio, and Pfizer; salary from the British Heart Foundation Intermediate Fellowship; share options in Lexeo Therapeutics; and shares in Mycardium. O.L. reports consultancy/advisory boards for Alnylam, Amicus Therapeutics, AstraZeneca, Neurimmune and Pfizer. O.A. serves on advisory boards for Alnylam Pharmaceuticals; speaker fees for Alnylam Pharmaceuticals and Pfizer; congress activities for Alnylam Pharmaceuticals, AstraZeneca and Pfizer; and clinical trial investigator for Alnylam Pharmaceuticals, AstraZeneca and Novo Nordisk. C.M. reports research cooperation with the University of Würzburg and Tomtec Imaging Systems funded by a research grant from the Bavarian Ministry of Economic Affairs, Regional Development and Energy, Germany; advisory and

speakers honoraria as well as travel grants from Amgen, Tomtec, Alnylam, Sobi, Alexion, Janssen, Pfizer and EBR Systems; principal investigator in trials sponsored by Alnylam, AstraZeneca and Bayer. S.B., P.Y.J. and J.V. are employees of Alnylam Pharmaceuticals and report ownership of equity in Alnylam Pharmaceuticals. S.D.S. reports research grants from Alexion, Alnylam Pharmaceuticals, Applied Therapeutics, AstraZeneca, Bayer, Bellerophon, BMS, Boston Scientific, Cytokinetics, Edgewise, Eidos/Bridgebio, Gossamer, GSK, Ionis, Lilly, NIH/NHLBI, Novartis, Novo Nordisk, Respicardia, Sanofi Pasteur, Tenaya, Theracos, and Us2.ai; and has consulted for Abbott, Action, Akros, Alexion, Alnylam Pharmaceuticals, American Regent, Amgen, Anacardio, Arena, AstraZeneca, Bayer, BMS, Cardior, Cardurion, CellProThera, Corvia, Cytokinetics, Dinaqor, GSK, Lexicon, Lilly, Moderna, Novartis, Quantum Genomics, Roche, Sanofi Pasteur, Sarepta, Tenaya, Theracos, Trembeau and Valo. The remaining authors declare no competing interests.

Additional information

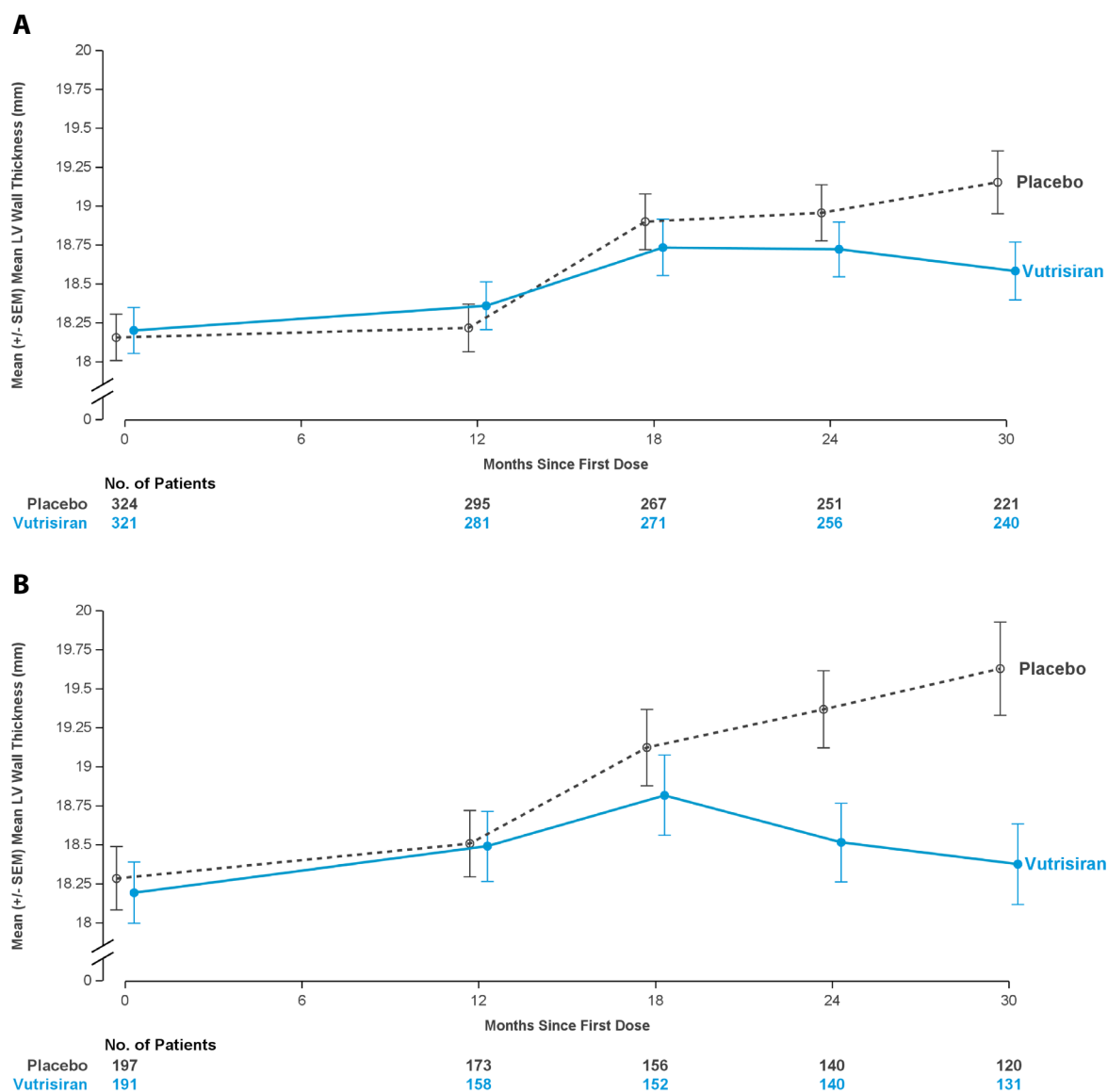
Extended data is available for this paper at <https://doi.org/10.1038/s41591-025-03851-z>.

Supplementary information The online version contains supplementary material available at <https://doi.org/10.1038/s41591-025-03851-z>.

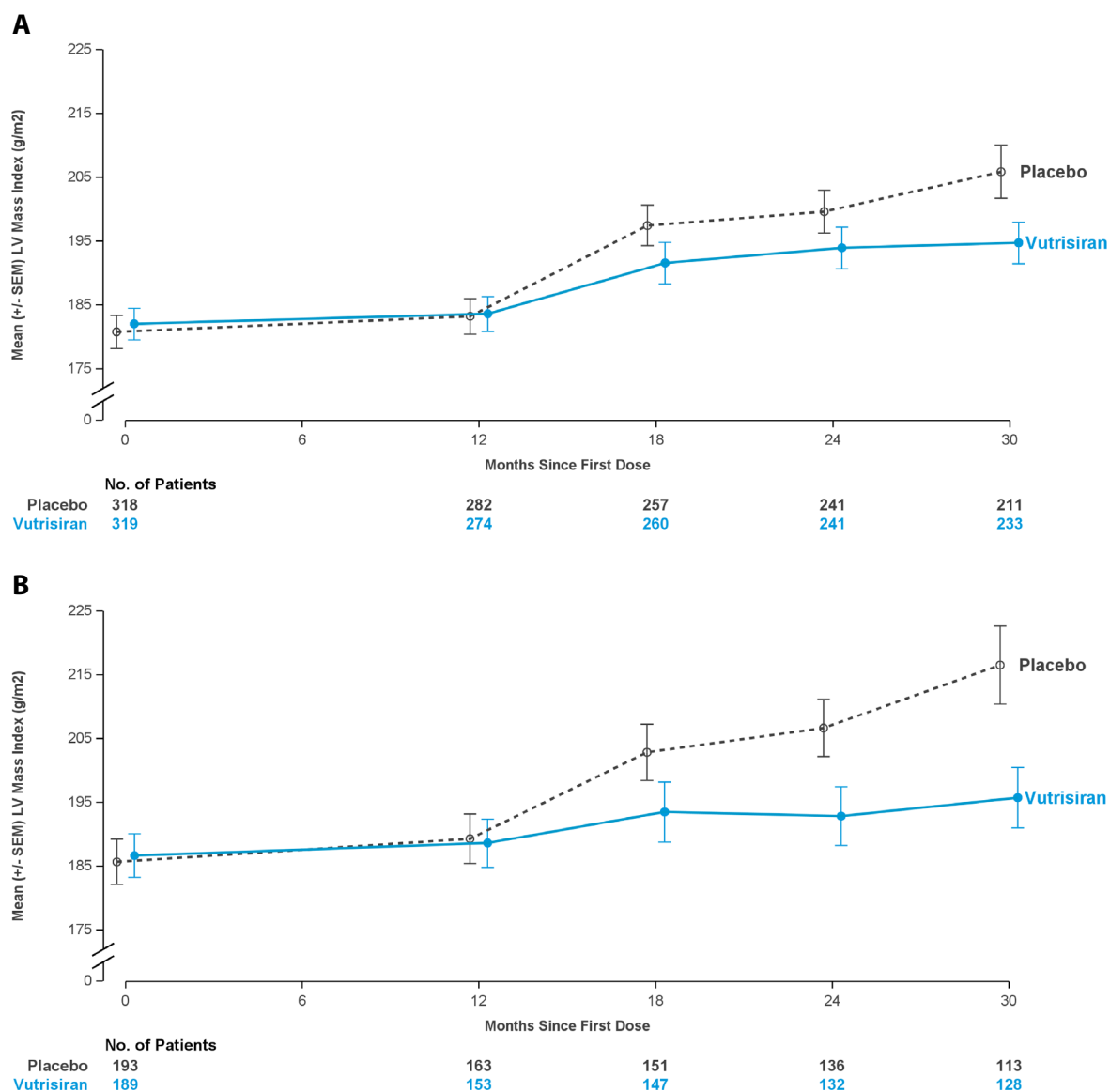
Correspondence and requests for materials should be addressed to Scott D. Solomon.

Peer review information *Nature Medicine* thanks Diana Bonderman, Prem Soman and the other, anonymous, reviewer(s) for their contribution to the peer review of this work. Primary Handling Editor: Michael Basson, in collaboration with the *Nature Medicine* team.

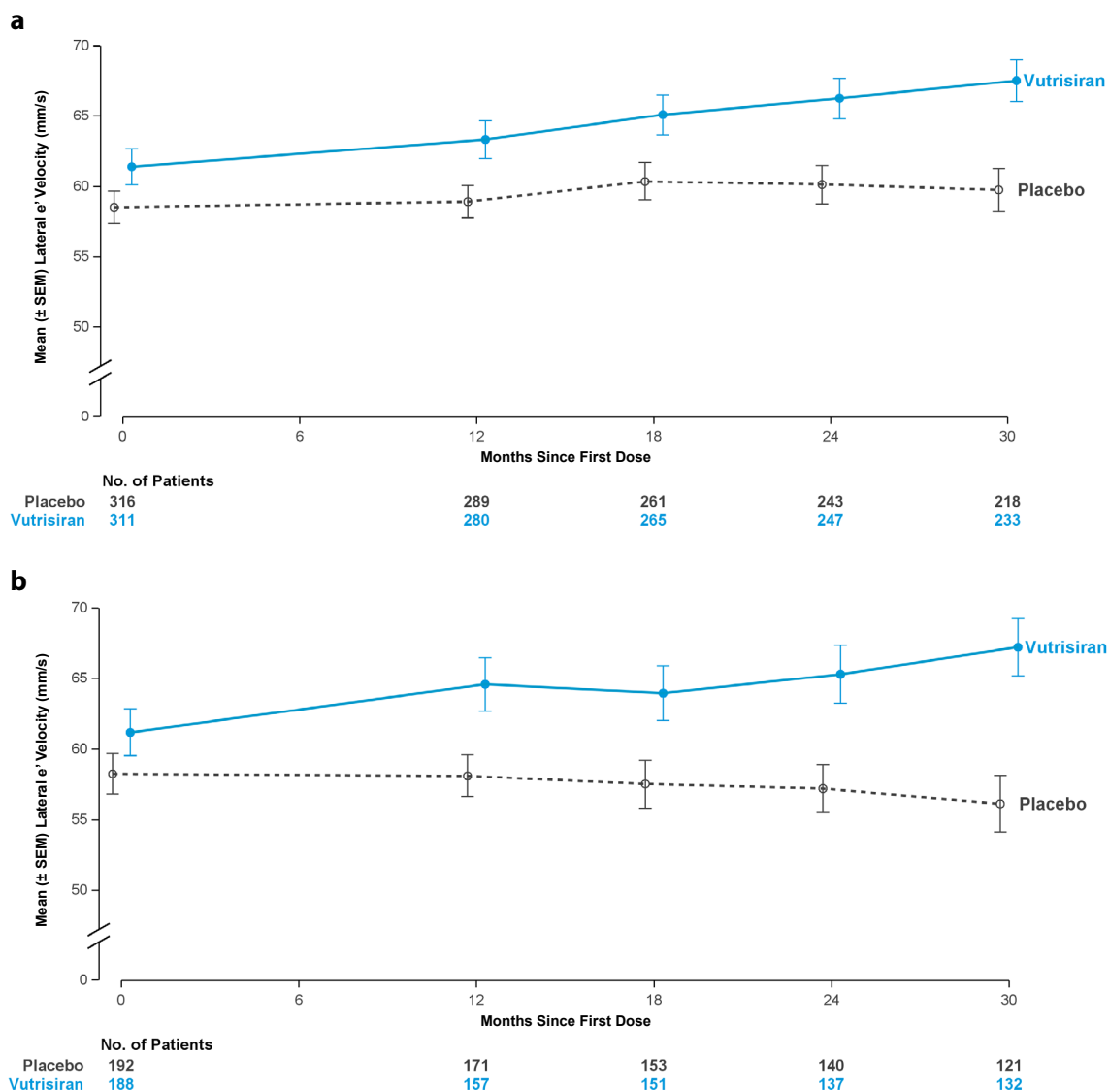
Reprints and permissions information is available at www.nature.com/reprints.



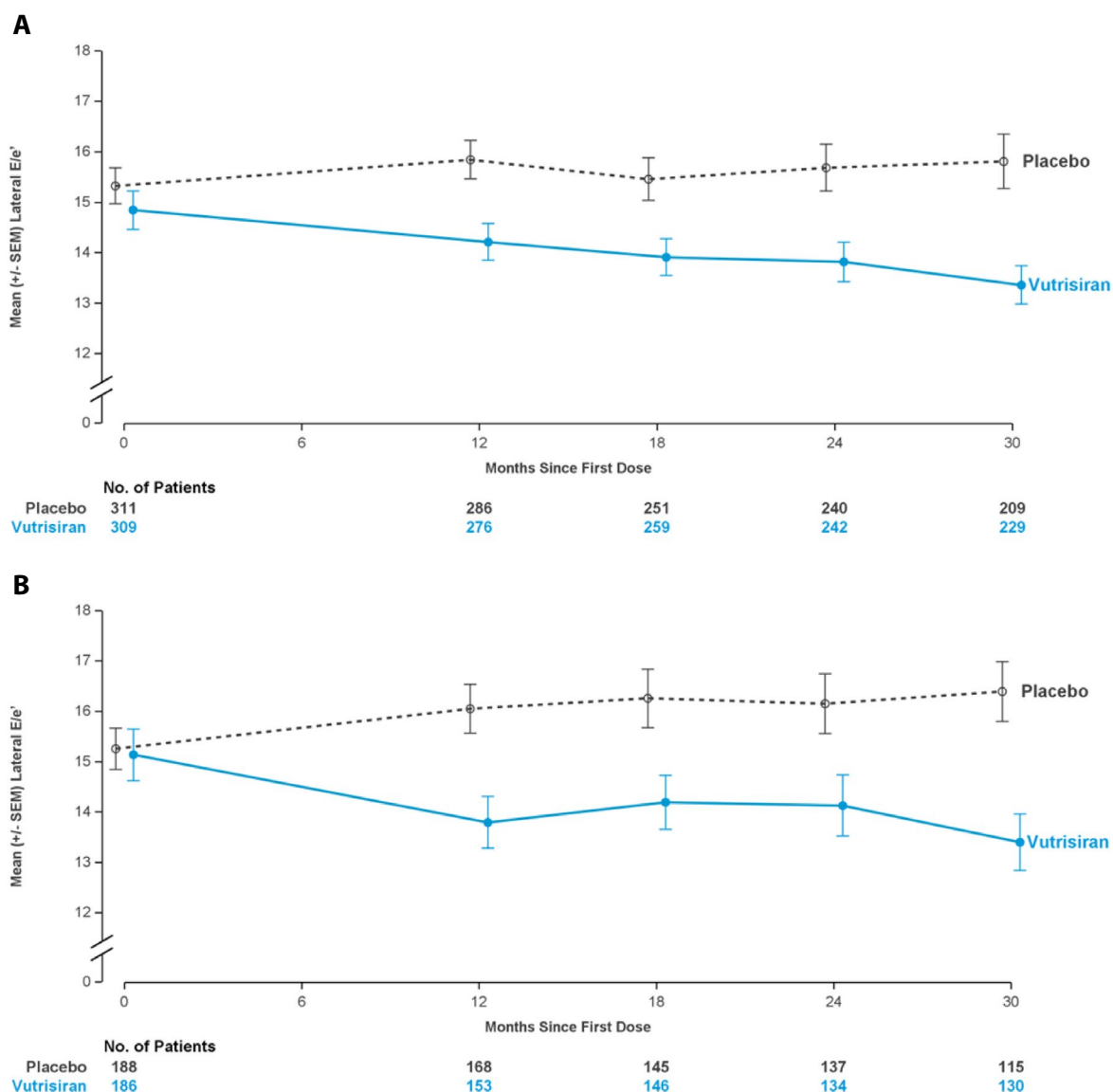
Extended Data Fig. 1 | Effect of Vutrisiran on Mean Left Ventricular Wall Thickness Over Time. Mean values (\pm SEM) during follow-up are shown according to treatment assignment in the (a) overall ($n = 645$) and (b) vutrisiran monotherapy population ($n = 388$). Error bars represent the standard error of the mean.



Extended Data Fig. 2 | Effect of Vutrisiran on Left Ventricular Mass Index Over Time. Mean values (\pm SEM) during follow-up are shown according to treatment assignment in the (a) overall ($n = 637$) and (b) vutrisiran monotherapy population ($n = 382$). Error bars represent the standard error of the mean.

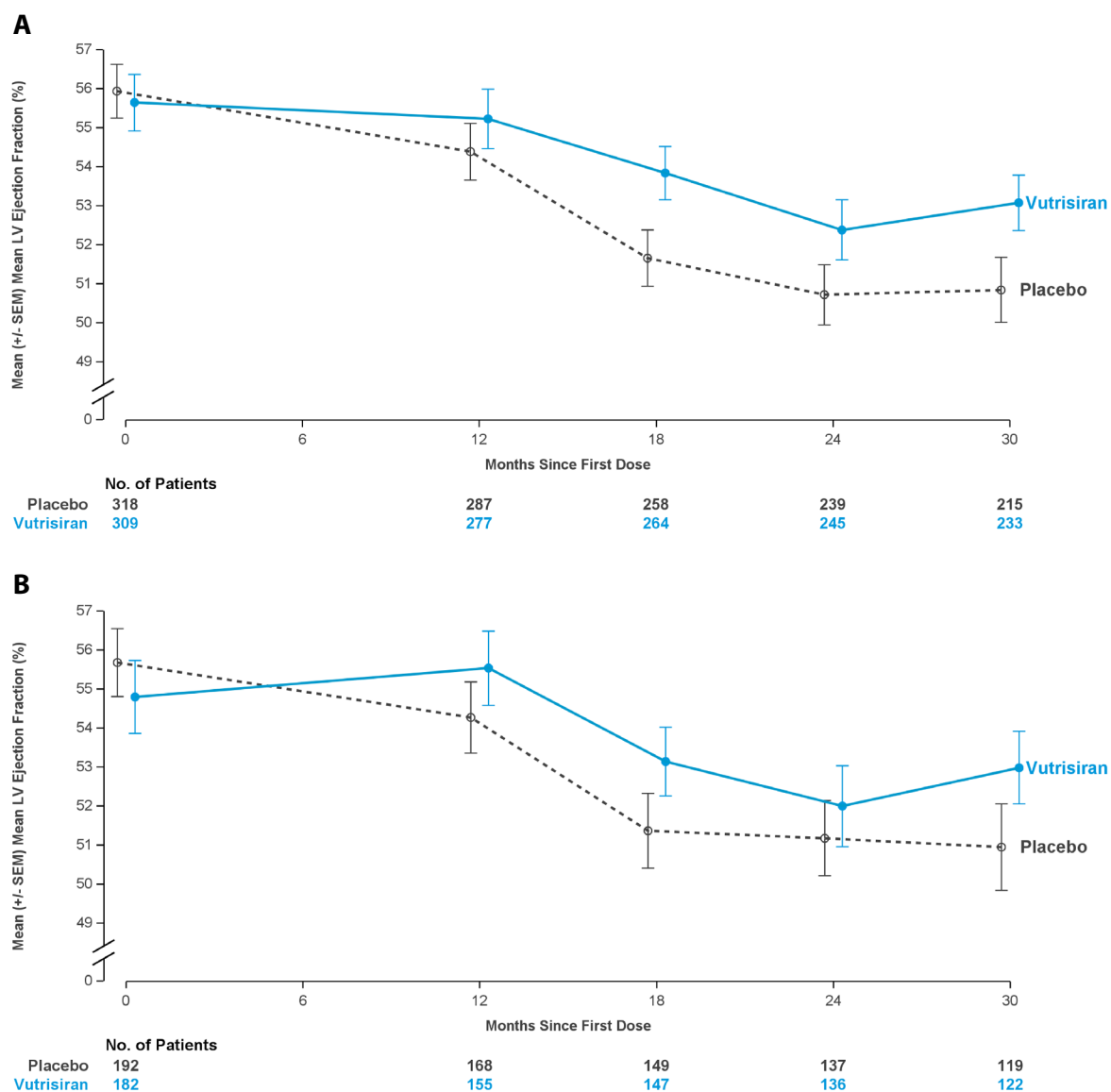


Extended Data Fig. 3 | Effect of Vutrisiran on Lateral Early Diastolic Mitral Annular Tissue Velocity (e') Over Time. Mean values (\pm SEM) during follow-up are shown according to treatment assignment in the (a) overall ($n = 627$) and (b) vutrisiran monotherapy population ($n = 380$). Error bars represent the standard error of the mean.

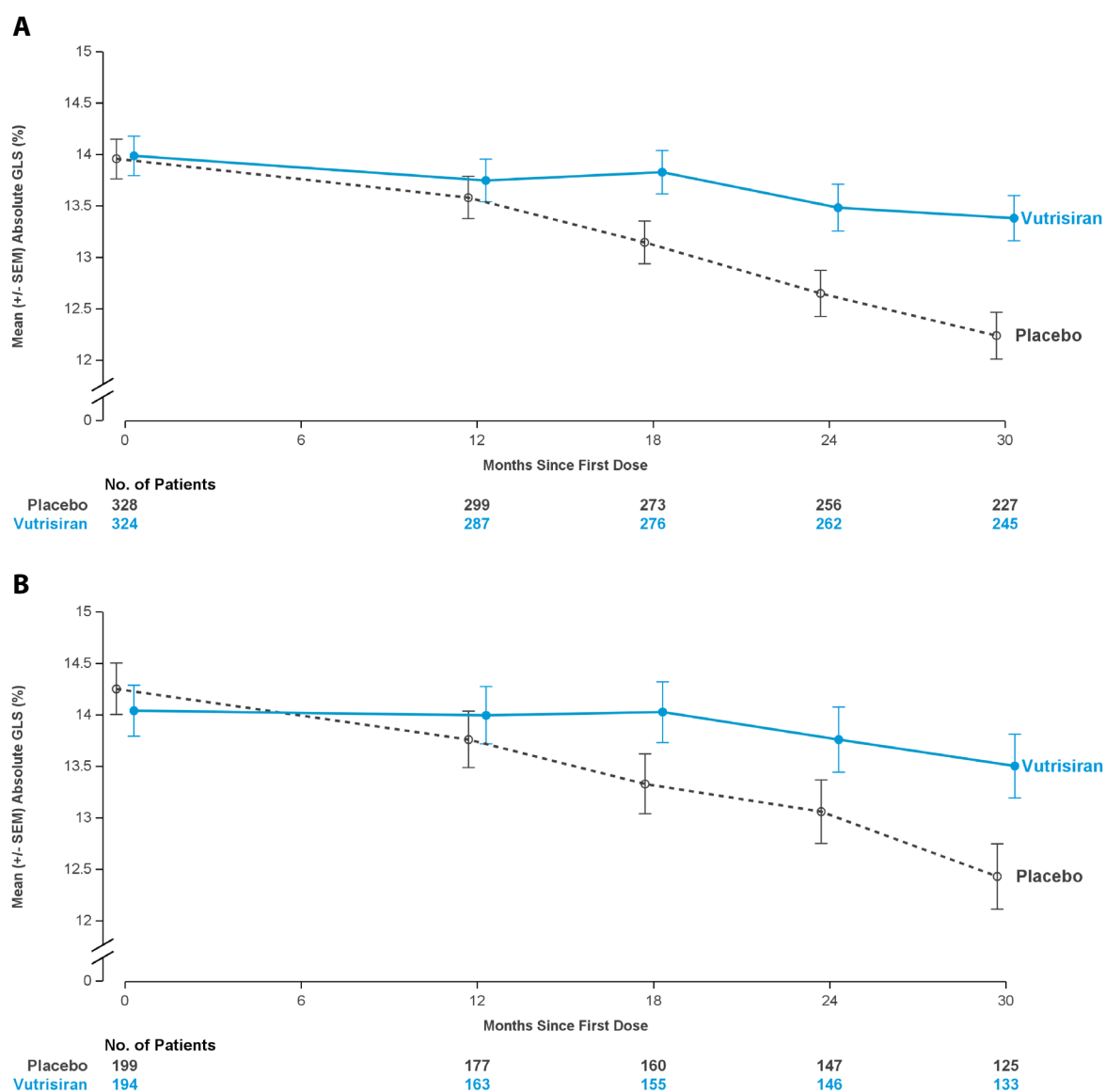


Extended Data Fig. 4 | Effect of Vutrisiran on the Ratio of Early Diastolic Transmitral Flow Velocity to Lateral Early Diastolic Mitral Annular Tissue Velocity (E/e') Over Time. Mean values (\pm SEM) during follow-up are shown

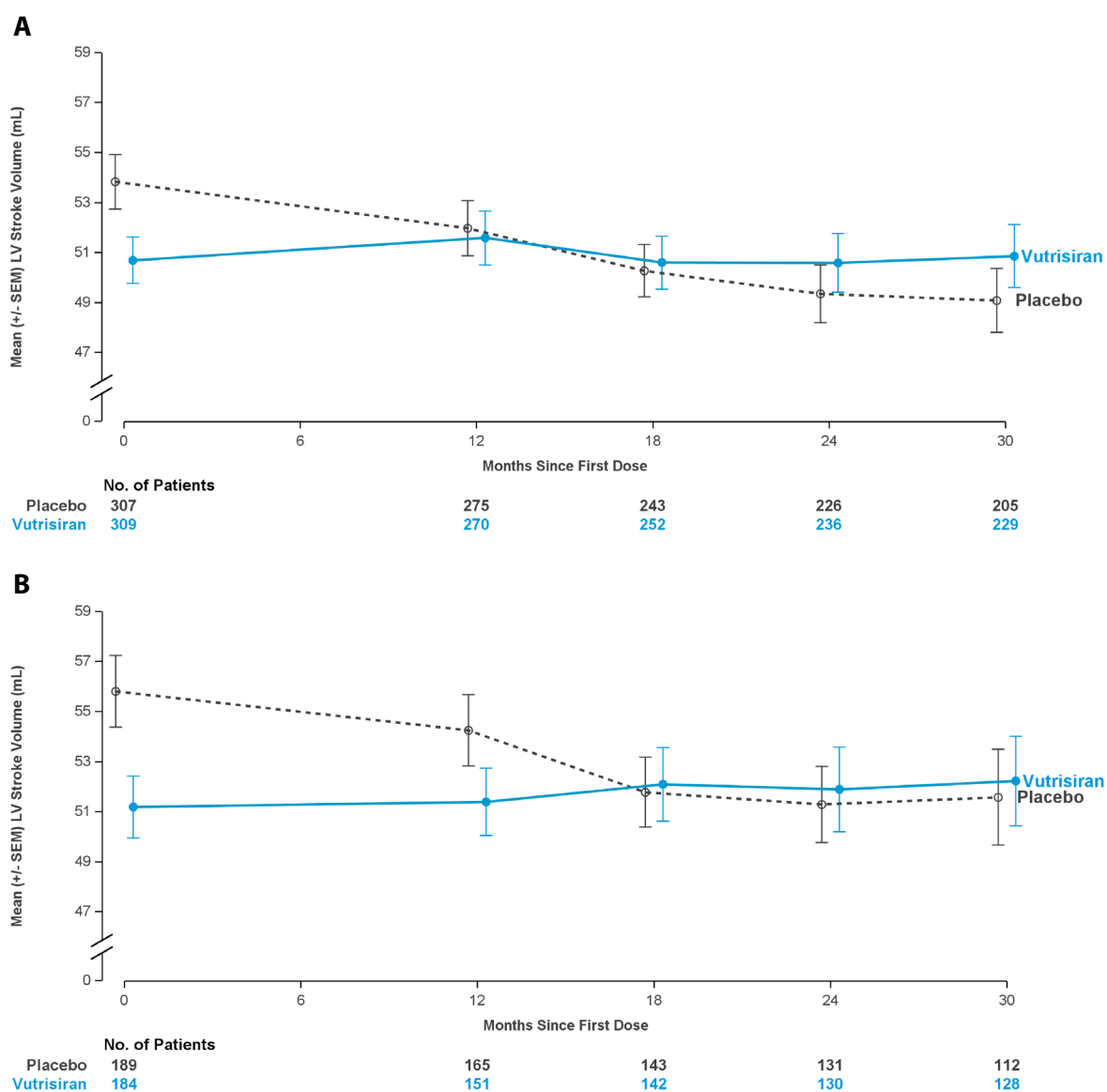
according to treatment assignment in the (a) overall ($n = 620$) and (b) vutrisiran monotherapy population ($n = 321$). Error bars represent the standard error of the mean.



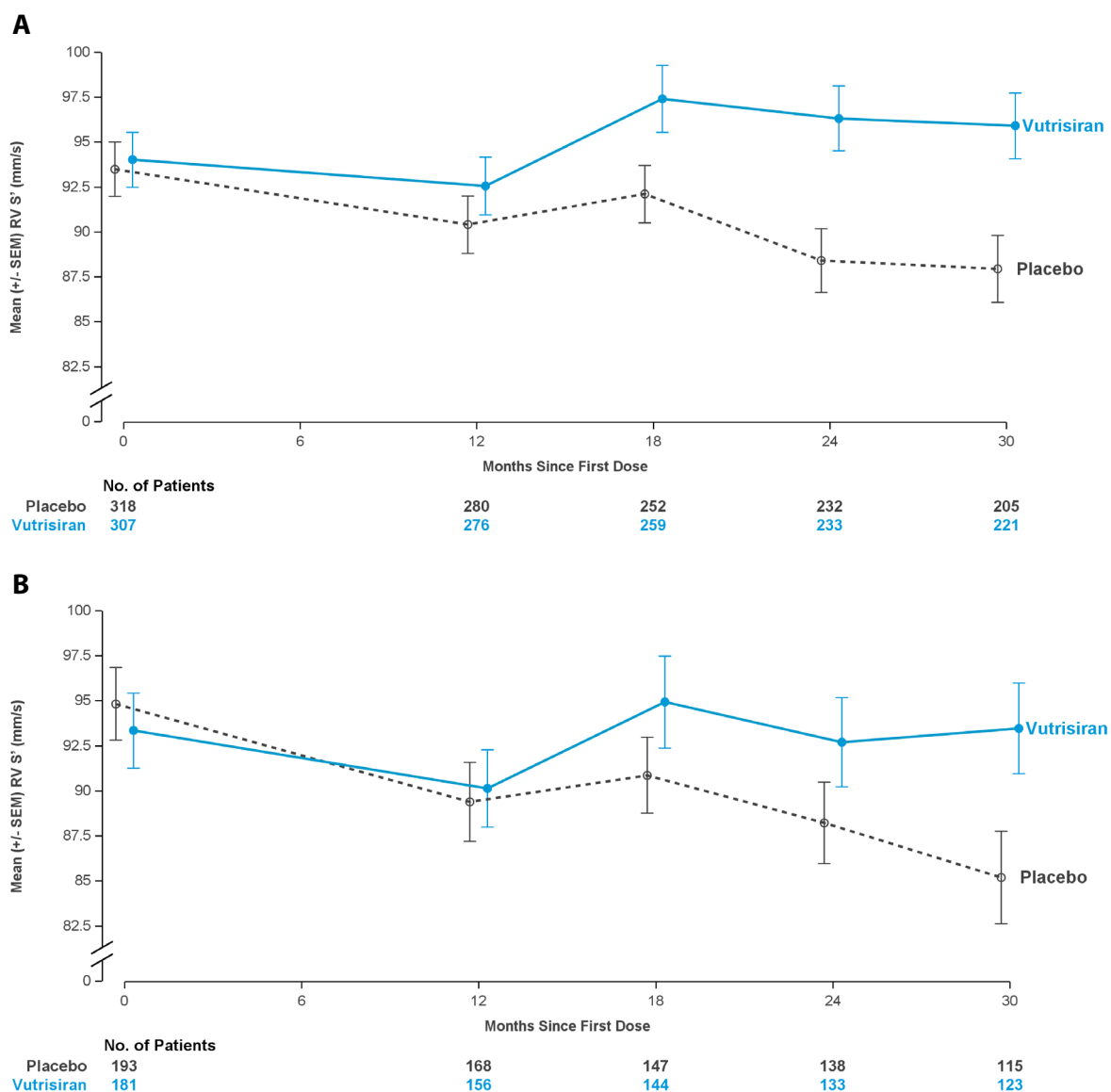
Extended Data Fig. 5 | Effect of Vutrisiran on Left Ventricular Ejection Fraction Over Time. Mean values (\pm SEM) during follow-up are shown according to treatment assignment in the (a) overall ($n = 627$) and (b) vutrisiran monotherapy population ($n = 374$). Error bars represent the standard error of the mean.



Extended Data Fig. 6 | Effect of Vutrisiran on Absolute Global Longitudinal Strain Over Time. Mean values (\pm SEM) during follow-up are shown according to treatment assignment in the (a) overall ($n = 652$) and (b) vutrisiran monotherapy population ($n = 393$). Error bars represent the standard error of the mean.



Extended Data Fig. 7 | Effect of Vutrisiran on Left Ventricular Stroke Volume Over Time. Mean values (\pm SEM) during follow-up are shown according to treatment assignment in the (a) overall ($n = 616$) and (b) vutrisiran monotherapy population ($n = 373$). Error bars represent the standard error of the mean.



Extended Data Fig. 8 | Effect of Vutrisiran on Tricuspid Annular Systolic Myocardial Velocity (RV S') Over Time. Mean values (\pm SEM) during follow-up are shown according to treatment assignment in the (a) overall ($n = 625$) and (b) vutrisiran monotherapy population ($n = 374$). Error bars represent the standard error of the mean.

Extended Data Table 1 | Baseline Demographics and Disease Characteristics According to Treatment Assignment and Underlying Tafamidis Treatment

Characteristic	Overall Population		Vutrisiran Monotherapy Population	
	Placebo n = 328	Vutrisiran n = 326	Placebo n = 199	Vutrisiran n = 196
Median age (range), years	76.0 (46-85)	77.0 (45-85)	76.0 (53-85)	77.5 (46-85)
Male sex (%)	306 (93)	299 (92)	183 (92)	178 (91)
Race (%)				
White	275 (84)	277 (85)	169 (85)	169 (86)
Asian	19 (6)	18 (6)	15 (8)	12 (6)
Black	24 (7)	23 (7)	11 (6)	10 (5)
Other or not reported	10 (3)	8 (2)	4 (2)	5 (3)
Wild-type ATTR (%)	289 (88)	289 (89)	174 (87)	173 (88)
Median time since diagnosis of ATTR (range), years	1.0 (0-10.8)	0.9 (0-11.1)	0.6 (0-6.2)	0.5 (0-8.3)
Tafamidis use at baseline (%)	129 (39%)	130 (40%)	--	--
NYHA functional class (%)				
I	35 (11)	49 (15)	12 (6)	15 (8)
II	258 (79)	250 (77)	169 (85)	172 (88)
III	35 (11)	27 (8)	18 (9)	9 (5)
NAC stage (%)*				
1	229 (70)	208 (64)	138 (69)	113 (58)
2	87 (27)	100 (31)	55 (28)	68 (35)
3	12 (4)	18 (6)	6 (3)	15 (8)
Mean 6-MWT, m (SD)	377.1 (96.3)	372.0 (103.7)	372.8 (98.1)	362.7 (102.7)
Mean KCCQ-OS (SD)	72.3 (19.9)	73.0 (19.4)	69.9 (20.8)	70.3 (20.2)
<i>Laboratory parameters, median (IQR)</i>				
NT-proBNP, pg/mL	1801 (1042-3082)	2021 (1138-3312)	1865 (1067-3099)	2402 (1322-3868)
High-sensitivity troponin I, pg/mL	65.2 (41.1-105.5)	71.9 (44.9-115.9)	62.2 (39.2-105.6)	76.3 (48.4-138.8)
<i>Coexisting conditions (%)</i>				
Hypertension	187 (57)	185 (57)	111 (56)	107 (55)
Diabetes	55 (17)	56 (17)	39 (20)	35 (18)
Atrial fibrillation	196 (60)	197 (60)	111 (56)	115 (59)

Values are n (%), mean \pm SD, or median (IQR). Race was self-reported. *NAC stage classifies patients according to NT-proBNP and eGFR levels: Stage 1 (lower risk) is defined as NT-proBNP \leq 3000 pg/mL and eGFR \geq 45 mL/min/1.73 m²; stage 2 (intermediate risk) includes patients not meeting stage 1 or 3 criteria; stage 3 (higher risk) is defined as NT-proBNP 3000 pg/mL and eGFR \geq 45 mL/min/1.73 m². 6-MWT – 6-minute walk test, ATTR – transthyretin amyloidosis, eGFR – estimated glomerular filtration rate, IQR – interquartile range, KCCQ-OS – Kansas City Cardiomyopathy Questionnaire-Overall Summary; NAC – National Amyloidosis Centre; NT-proBNP – N-terminal pro-B-type natriuretic peptide, NYHA – New York Heart Association, SD – standard deviation.

Extended Data Table 2 | Placebo-Corrected Treatment Difference at Month 30 with and without Imputation for Missing Data for Selected Echocardiographic Variables in the Overall Population

Echocardiographic parameters	Repeated Measures Model	Pattern Mixture Model
	LS mean difference (95% CI)	LS mean difference (95% CI)
<i>LV structure</i>		
Mean LV wall thickness (mm)	-0.4 (-0.8, -0.0)	-0.5 (-1.0, -0.1)
LV mass index (g/m ²)	-10.6 (-18.0, -3.3)	-17.2 (-26.3, -8.1)
<i>LV systolic function</i>		
LVEF (%)	2.0 (0.3, 3.7)	3.1 (1.2, 5.1)
Absolute global longitudinal strain (%)	1.2 (0.7, 1.7)	1.3 (0.7, 1.9)
Stroke volume (mL)	4.1 (1.7, 6.4)	5.3 (2.7, 7.9)
TDI lateral s' (mm/s)	4.6 (2.1, 7.2)	5.3 (2.2, 8.3)
TDI septal s' (mm/s)	3.8 (1.9, 5.6)	4.6 (2.5, 6.8)
<i>LV diastolic function</i>		
TDI lateral e' (mm/s)	5.5 (2.4, 8.5)	6.0 (2.5, 9.4)
TDI septal e' (mm/s)	3.8 (1.8, 5.8)	4.9 (2.6, 7.1)
Average E/e'	-2.0 (-2.9, -1.2)	-2.5 (-3.5, -1.4)
<i>Left atrial function</i>		
TDI lateral a' (mm/s)	4.0 (-0.1, 8.0)	5.2 (0.8, 9.6)
TDI septal a' (mm/s)	3.0 (-0.8, 6.9)	3.0 (-1.2, 7.2)
<i>Right ventricle</i>		
Tricuspid annular systolic myocardial velocity (S') (mm/s)	7.0 (2.8, 11.2)	8.5 (3.5, 13.5)

a' – peak late diastolic mitral annular tissue velocity, e' – peak early diastolic mitral annular tissue velocity, E wave – peak early diastolic transmitral flow velocity, LV – left ventricular, LVEF – left ventricular ejection fraction, s' – peak systolic mitral annular tissue velocity, TDI – tissue Doppler imaging.

Reporting Summary

Nature Portfolio wishes to improve the reproducibility of the work that we publish. This form provides structure for consistency and transparency in reporting. For further information on Nature Portfolio policies, see our [Editorial Policies](#) and the [Editorial Policy Checklist](#).

Statistics

For all statistical analyses, confirm that the following items are present in the figure legend, table legend, main text, or Methods section.

n/a	Confirmed
<input type="checkbox"/>	<input checked="" type="checkbox"/> The exact sample size (<i>n</i>) for each experimental group/condition, given as a discrete number and unit of measurement
<input checked="" type="checkbox"/>	<input type="checkbox"/> A statement on whether measurements were taken from distinct samples or whether the same sample was measured repeatedly
<input type="checkbox"/>	<input checked="" type="checkbox"/> The statistical test(s) used AND whether they are one- or two-sided <i>Only common tests should be described solely by name; describe more complex techniques in the Methods section.</i>
<input type="checkbox"/>	<input checked="" type="checkbox"/> A description of all covariates tested
<input type="checkbox"/>	<input checked="" type="checkbox"/> A description of any assumptions or corrections, such as tests of normality and adjustment for multiple comparisons
<input type="checkbox"/>	<input checked="" type="checkbox"/> A full description of the statistical parameters including central tendency (e.g. means) or other basic estimates (e.g. regression coefficient) AND variation (e.g. standard deviation) or associated estimates of uncertainty (e.g. confidence intervals)
<input type="checkbox"/>	<input checked="" type="checkbox"/> For null hypothesis testing, the test statistic (e.g. <i>F</i> , <i>t</i> , <i>r</i>) with confidence intervals, effect sizes, degrees of freedom and <i>P</i> value noted <i>Give P values as exact values whenever suitable.</i>
<input checked="" type="checkbox"/>	<input type="checkbox"/> For Bayesian analysis, information on the choice of priors and Markov chain Monte Carlo settings
<input checked="" type="checkbox"/>	<input type="checkbox"/> For hierarchical and complex designs, identification of the appropriate level for tests and full reporting of outcomes
<input checked="" type="checkbox"/>	<input type="checkbox"/> Estimates of effect sizes (e.g. Cohen's <i>d</i> , Pearson's <i>r</i>), indicating how they were calculated

Our web collection on [statistics for biologists](#) contains articles on many of the points above.

Software and code

Policy information about [availability of computer code](#)

Data collection	Rave EDC version 2024.1.1. was used for case report form data collection. Echocardiographic measurements were performed using commercially available software (US2.ai versions 1.4 and 2.0).
Data analysis	Statistical analyses were performed using SAS version 9.4.

For manuscripts utilizing custom algorithms or software that are central to the research but not yet described in published literature, software must be made available to editors and reviewers. We strongly encourage code deposition in a community repository (e.g. GitHub). See the Nature Portfolio [guidelines for submitting code & software](#) for further information.

Data

Policy information about [availability of data](#)

- All manuscripts must include a [data availability statement](#). This statement should provide the following information, where applicable:
- Accession codes, unique identifiers, or web links for publicly available datasets
 - A description of any restrictions on data availability
 - For clinical datasets or third party data, please ensure that the statement adheres to our [policy](#)

Access to anonymized individual participant data that support these results is made available 12 months after study completion and not less than 12 months after the product and indication have been approved in the US and/or the EU. Access to data may be declined where there is likelihood a patient could be identified or other feasibility issue, where there is a potential conflict of interest, planned business activities or an actual or potential competitive risk. Data will be provided

contingent upon the approval of a research proposal and the execution of a data sharing agreement. Timeframes for data access may vary and can take up to 6 months or more. Requests for access to data can be submitted via the website www.vivli.org. Questions can also be directed to datasharing@alnylam.com.

Research involving human participants, their data, or biological material

Policy information about studies with [human participants or human data](#). See also policy information about [sex, gender \(identity/presentation\), and sexual orientation](#) and [race, ethnicity and racism](#).

Reporting on sex and gender

The n (%) of males/females was described overall and by randomized therapy. Sex was self-reported. Heterogeneity of treatment effect by sex was not evaluated due to the relatively low number of women enrolled in HELIOS-B, consistent with the reported demographic characteristics of patients with ATTR-CM. Given the male preponderance of patients with ATTR-CM, power to estimate treatment effects according to sex was limited.

Reporting on race, ethnicity, or other socially relevant groupings

The n (%) of each racial category (White, Asian, Black, Other) was described by randomized therapy. Race was self-reported.

Population characteristics

Patients 18–85 years of age with a diagnosis of either variant or wild-type ATTR-CM established on the basis of tissue biopsy or validated scintigraphy-based diagnostic criteria with evidence of cardiac involvement (interventricular septal wall thickness >12 mm on echocardiography) and a clinical history of symptomatic HF. Median (interquartile range [IQR]) age was 77 years (45–85), 93% were male, 88% had wild-type ATTR-CM, 91% New York Heart Association functional class ≤ II and 67% National Amyloidosis Centre stage 1. Approximately 40% of patients were using tafamidis at baseline.

Recruitment

Participants were recruited from 87 sites across 26 countries. Participants were enrolled from academic/hospital-based or community health care facilities and per protocol could not have been hospitalized for cardiovascular reasons in the six weeks prior to randomization. All participants were required to meet specific inclusion and exclusion criteria, as specified in the study protocol, to be considered eligible for the trial and there was no self-selection. Effects of selection bias on the outcomes reported in this study were minimal given the randomized design.

Ethics oversight

The local ethics committee at each participating site approved the study protocol, and patients provided written informed consent in accordance with established guidelines. The complete list of committees that approved the HELIOS-B protocol is provided in the supplementary appendix.

Note that full information on the approval of the study protocol must also be provided in the manuscript.

Field-specific reporting

Please select the one below that is the best fit for your research. If you are not sure, read the appropriate sections before making your selection.

☒ Life sciences ☐ Behavioural & social sciences ☐ Ecological, evolutionary & environmental sciences

For a reference copy of the document with all sections, see nature.com/documents/nr-reporting-summary-flat.pdf

Life sciences study design

All studies must disclose on these points even when the disclosure is negative.

Sample size

Enrollment of 600 patients was planned and 654 patients were randomized, including 60% patients in the vutrisiran monotherapy group. Sample size was calculated based on the following assumptions such that the study would have approximately 80% power in both the overall population and the vutrisiran monotherapy group to detect a difference between treatment groups using a modified Andersen-Gill model with robust variance estimator, with a 2-sided alpha of 0.05:

- In the monotherapy subgroup, vutrisiran provides a 25% reduction in mortality rates and a 35% reduction in recurrent cardiovascular event rates compared with placebo over 30 months; 0.34 cardiovascular events per patient-year and 25% mortality rate at month 30 were assumed in the placebo group.
- In the background tafamidis subgroup, vutrisiran plus tafamidis provides a 10% reduction in mortality rates and a 15% reduction in recurrent cardiovascular event rates compared with placebo plus tafamidis over 30 months.
- A 9-month and 18-month delay to effect on cardiovascular events and death, respectively.
- In the vutrisiran monotherapy subgroup, approximately 20% of patients in both treatment arms add tafamidis anytime during the first 24 months on study.
- Cardiovascular events and mortality data will be collected up to 36 months and no more than 15% of patients in both treatment arms are lost to follow-up.

Data exclusions

Only patients with critical Good Clinical Practice violations or missing baseline echocardiograms were excluded.

Replication

Consistency in treatment effects for the primary and secondary endpoints was confirmed both in the overall study population and in the vutrisiran monotherapy group. For this study, echocardiographic measurements were performed in triplicates whenever possible and were averaged. In patients with atrial fibrillation, measurements were repeated five times and were averaged. Lab-wide intra- and interobserver variability for key measures of cardiac structure and function have been previously reported; (1-3) amongst analysts involved in this study the coefficient of variation was ≤16% and intraclass correlation ≥0.72.

1. Shah AM, Shah SJ, Anand IS, et al. Cardiac structure and function in heart failure with preserved ejection fraction: baseline findings from the echocardiographic study of the Treatment of Preserved Cardiac Function Heart Failure with an Aldosterone Antagonist trial. *Circulation: Heart Failure*. 2014;7(1):104-115.
2. Shah AM, Cheng S, Skali H, et al. Rationale and Design of a Multicenter Echocardiographic Study to Assess the Relationship Between Cardiac Structure and Function and Heart Failure Risk in a Biracial Cohort of Community-Dwelling Elderly Persons. *Circulation: Cardiovascular Imaging*. 2014;7(1):173-181. doi:doi:10.1161/CIRCIMAGING.113.000736
3. Kraigher-Krainer E, Shah AM, Gupta DK, et al. Impaired systolic function by strain imaging in heart failure with preserved ejection fraction. *J Am Coll Cardiol*. Feb 11 2014;63(5):447-56. doi:10.1016/j.jacc.2013.09.052

Randomization

Patients were randomized in a 1:1 ratio to receive 25 mg of vutrisiran or placebo administered subcutaneously every 12 weeks. Randomization was stratified by: 1) baseline tafamidis use (yes versus no); 2) ATTR disease type (variant versus wild-type ATTR amyloidosis with cardiomyopathy); and 3) New York Heart Association Class I or II and age <75 years versus all other.

Blinding

HELIOS-B was a double-blind, placebo-controlled randomized clinical trial. Specifically, all investigators remained strictly blinded to treatment arm allocation during data collection and analysis. Furthermore, echocardiograms were reviewed by dedicated analysts blinded to clinical characteristics of study participants, treatment assignment, and temporal sequence.

Reporting for specific materials, systems and methods

We require information from authors about some types of materials, experimental systems and methods used in many studies. Here, indicate whether each material, system or method listed is relevant to your study. If you are not sure if a list item applies to your research, read the appropriate section before selecting a response.

Materials & experimental systems

- | | |
|-------------------------------------|--|
| n/a | Involved in the study |
| <input checked="" type="checkbox"/> | <input type="checkbox"/> Antibodies |
| <input checked="" type="checkbox"/> | <input type="checkbox"/> Eukaryotic cell lines |
| <input checked="" type="checkbox"/> | <input type="checkbox"/> Palaeontology and archaeology |
| <input checked="" type="checkbox"/> | <input type="checkbox"/> Animals and other organisms |
| <input type="checkbox"/> | <input checked="" type="checkbox"/> Clinical data |
| <input checked="" type="checkbox"/> | <input type="checkbox"/> Dual use research of concern |
| <input checked="" type="checkbox"/> | <input type="checkbox"/> Plants |

Methods

- | | |
|-------------------------------------|---|
| n/a | Involved in the study |
| <input checked="" type="checkbox"/> | <input type="checkbox"/> ChIP-seq |
| <input checked="" type="checkbox"/> | <input type="checkbox"/> Flow cytometry |
| <input checked="" type="checkbox"/> | <input type="checkbox"/> MRI-based neuroimaging |

Clinical data

Policy information about [clinical studies](#)

All manuscripts should comply with the ICMJE [guidelines for publication of clinical research](#) and a completed [CONSORT checklist](#) must be included with all submissions.

Clinical trial registration

NCT04153149

Study protocol

The study protocol and statistical analysis plan were published with the primary paper in NEJM (Fontana M, Berk JL, Gillmore JD, et al. Vutrisiran in Patients with Transthyretin Amyloidosis with Cardiomyopathy. *N Engl J Med*. Aug 30 2024;doi:10.1056/NEJMoa2409134).

Data collection

Participants in HELIOS-B were enrolled from December 2019 through August 2021 at 87 sites across 26 countries. Participants were enrolled from academic/hospital-based or community health care facilities and per protocol could not have been hospitalized for cardiovascular reasons in the preceding six weeks. A list of participating sites is included in the supplementary appendix.

Outcomes

The prespecified primary endpoint of HELIOS-B was a composite of all-cause death and recurrent cardiovascular events (defined as hospitalizations for cardiovascular causes or urgent visits for heart failure) during the double-blind period (up to 36 months). Clinical outcomes were adjudicated by an independent clinical events committee blinded to treatment assignment. Changes in cardiac structure and function (change from baseline in mean left ventricular wall thickness and global longitudinal strain) were prespecified as an outcome of interest in the study protocol and statistical analysis plan. Secondary outcomes including changes from baseline to month 30 in echocardiographic measures of cardiac structure and function (mean left ventricular wall thickness and global longitudinal strain) were pre-specified in the study protocol and statistical analysis plan.

Per protocol, certified sonographers at each site performed serial echocardiograms at baseline, month 12, 18, 24 and 30. Echocardiographic images were transferred to the Cardiovascular Imaging Core Laboratory (Brigham and Women's Hospital, Boston, MA, USA) and were evaluated by dedicated analysts blinded to clinical characteristics of study participants, randomized treatment assignment and temporal sequence. Echocardiographic measurements were performed in triplicate (five times for participants in atrial fibrillation) and were averaged. Measurements were performed using commercially available software (US2ai version 1.4 and 2.0, Singapore, Singapore) in accordance with American Society of Echocardiography guidelines.

Seed stocks	Report on the source of all seed stocks or other plant material used. If applicable, state the seed stock centre and catalogue number. If plant specimens were collected from the field, describe the collection location, date and sampling procedures.
Novel plant genotypes	Describe the methods by which all novel plant genotypes were produced. This includes those generated by transgenic approaches, gene editing, chemical/radiation-based mutagenesis and hybridization. For transgenic lines, describe the transformation method, the number of independent lines analyzed and the generation upon which experiments were performed. For gene-edited lines, describe the editor used, the endogenous sequence targeted for editing, the targeting guide RNA sequence (if applicable) and how the editor was applied.
Authentication	Describe any authentication procedures for each seed stock used or novel genotype generated. Describe any experiments used to assess the effect of a mutation and, where applicable, how potential secondary effects (e.g. second site T-DNA insertions, mosaicism, off-target gene editing) were examined.